Waste Management 214 (2026) 115406

Contents lists available at ScienceDirect

Waste Management

journal homepage: www.elsevier.com/locate/wasman

Research Paper

# Comprehensive study of physicochemical and environmental properties of Air pollution control residues from UK energy-from-waste facilities

Ximena Chamorro Bolaños [a,*], Bamdad Ayati [a], Darryl Newport [b]

[a] Sustainability Research Institute (SRI), University of East London (UEL), Royal Docks Centre for Sustainability, Docklands Campus, 4 – 6 University Way, London E16 2RD, UK
[b] Suffolk Sustainability Institute, University of Suffolk, Waterfront Building, 19 Neptune Quay, Ipswich IP4 1QJ, UK

ARTICLE INFO

*Keywords:*
Municipal Solid Waste incineration
Air Pollution Control Residues
Hazardous waste
Leaching properties
Waste Acceptance Criteria
Mineral phase

ABSTRACT

Thermal treatment of Municipal Solid Waste in Energy-from-Waste (EfW) facilities enables energy recovery and landfill reduction but generates hazardous air pollution control residues (APCr). This study characterised 42 APCr samples from 22 UK EfW facilities, integrating compositional, mineralogical, leaching organic fraction and microstructural analyses to assess environmental implications. Scanning Electron Microscopy – Energy Dispersive X-Ray Spectroscopy (SEM-EDS) identified major elements (>0.1 wt%): O, Ca, Cl, Si, Al, Mg, Fe, K, Na, P, S and Zn. Inductively Coupled Plasma – Optical Emission Spectroscopy quantified total metal concentrations (mg/kg): Zn (>1,000), Cu and Pb (>100), As, Ba, Cd, Cr, Ni and Sb (< 1,000) and Mo (<100). X-Ray Diffraction identified 45 mineral phases, including 21 newly reported in APCr. Dominant phases comprised $CaSO_4$, $CaCO_3$, CaOHCl, $Ca(OH)_2$, NaCl, KCl and $SiO_2$, alongside Si-bearing phases, such as clinotobermorite ($Ca_5H_8O_{21}Si_6$) and sanidine ($KAlSi_3O_8$). Leaching tests showed environmental risks from Pb, Ba, Mo, Cr, Zn, Cu, chlorides and sulphates, with Pb and chlorides mostly exceeding hazardous Waste Acceptance Criteria (WAC). Organic indices showed Total Organic Carbon predominantly undetected, Loss on Ignition mostly below hazardous WAC and Dissolved Organic Carbon absent in most leachates, indicating that organics largely remain within the solid phase. SEM imaging revealed fine-grained material (0.1–1 µm), diverse particle morphologies and inclusions of unburnt organics, carbon and metals. Findings inform APCr treatment strategies for safe handling, recycling and resource recovery.

## 1. Introduction

### 1.1. Background

Management of Municipal Solid Waste (MSW) relies on landfilling, recycling and incineration, with incineration offering energy recovery in Energy-from-Waste (EfW) facilities. Waste incineration transfers hazardous substances to flue gases, requiring treatment to prevent environmental pollution. Air pollution control (APC) technologies, including scrubbers and electrostatic precipitators, remove particulates, generating solid by-products known as Air Pollution Control Residues (APCr). These residues, collected after reagent injection and before gas discharge (Chandler et al., 1997; Sawell et al., 1995), are classified as hazardous waste under code 19 01 07 of the European Waste Catalogue (European Union, 2023) due to their pollutant contents that pose leaching risks to soil and water in areas surrounding landfills. In the UK, APCr must meet Waste Acceptance Criteria (WAC) under the Landfill Directive (European Union, 2003), assessed through Loss on Ignition (LOI) and Total Organic Carbon (TOC) in the solid matrix, and leachable concentrations of heavy metals, soluble salts, Total Dissolved Solids (TDS) and Dissolved Organic Carbon (DOC). Comprehensive APCr characterisation is therefore essential for safe management and reuse.

---

*Abbreviations:* APC, Air Pollution Control; APCr, Air Pollution Control Residues; BEI, Backscatter Electron Imaging; CVs, Coefficients of Variation; DOC, Dissolved Organic Carbon; DTG, Derivative Thermogravimetry; EDS, Energy Dispersive X-Ray Spectroscopy; EfW, Energy from Waste; FTIR, Fourier Transform Infrared Spectroscopy; ICP-AES, Inductively Coupled Plasma – Atomic Emission Spectroscopy; ICP-OES, Inductively Coupled Plasma – Optical Emission Spectroscopy; ICP-MS, Inductively Coupled Plasma – Mass Spectrometry; LOI, Loss on ignition; MSW, Municipal Solid Waste; POPs, Persistent Organic Pollutants; SEI, Secondary Electron Imaging; SEM, Scanning Electron Microscopy; STA, Simultaneous Thermal Analysis; TOC, Total Organic Carbon; NDIR, Non-Dispersive Infrared Detector; TDS, Total Dissolved Solids; WAC, Waste Acceptance Criteria; XRD, X-Ray Diffraction; XRF, X-Ray Fluorescence.

* Corresponding author.
*E-mail address:* Ximena.Chamorro@bomidot.com (X. Chamorro Bolaños).

https://doi.org/10.1016/j.wasman.2026.115406
Received 16 October 2025; Received in revised form 7 February 2026; Accepted 10 February 2026

Existing UK studies have examined elemental composition, mineralogy and physicochemical properties, but WAC-regulated parameters remain insufficiently addressed. Moreover, the dynamic nature of MSW, heterogeneity of EfW facilities and APC technologies, and rising APCr volumes underscore the need for updated characterisation based on representative cross-sampling. Adaptive analytical frameworks are required to ensure accurate assessments and support evidence-based decisions on APCr management and reuse.

To address existing gaps in UK APCr characterisation, this study presents a comprehensive analysis of APCr generated in EfW facilities nationwide. It provides novel and updated insights into elemental composition, total metal contents, mineralogy, total mineral and amorphous fractions, estimated organic matter content, microstructure and leaching behaviour. All parameters were evaluated qualitatively and quantitatively, and regulated parameters were compared against WAC thresholds for hazardous waste. The findings are discussed in relation to how the microstructure and chemical properties of UK APCr influence their environmental impact post-landfilling, and their potential for recycling and resource recovery. This level of detail offers a robust foundation for developing effective treatment strategies that mitigate environmental risks and enhance material valorisation. Furthermore, a deeper understanding of compositional variability across APCr samples can inform strategic treatment pathways, such as processing mixed APCr streams at a single waste management facility or implementing targeted treatments to specific streams to optimise outcomes like metal recovery, particularly where distinct enrichment profiles are observed. This research is based on a batch of APCr samples sourced from multiple fully operational EfW facilities, selected to reflect the current scale, diversity and evolving nature of APCr production in the UK.

### *1.2. Characterisation of APCr in the UK: Current insights and gaps*

The characterisation of UK-produced APCr has been addressed in various studies with different objectives, but it was rarely the primary focus, as most research centred on treatments to improve recyclability, as summarised in Table 1. Of nine studies reviewed, five addressed elemental composition, mineralogy and microstructure, key factors for developing treatment strategies. These works highlighted metal concentrations and mineral phases associated with leaching behaviour but did not assess WAC compliance. The remaining four studies included some WAC-regulated parameters, yet none performed full characterisation contrasted against WAC thresholds. No study in the past 14 years has conducted WAC compliance testing on APCr. This omission is concerning, since understanding environmental properties is essential for safe management and recycling. Without compliance data, new products incorporating APCr may exhibit unsuitable leaching behaviour, lcomimiting regulatory acceptance, restricting applications and posing environmental risks.

The elemental composition of UK APCr has been investigated in most studies in Table 1, providing qualitative and quantitative data. These consistently report major elements (>1,000 mg/kg; 0.1 wt%), including Al, Ca, F, Fe, Cl, Mg, K, Na, P, Pb, S, Si, Ti and Zn. Since many elements occur as oxides, oxygen is also major, as noted by Hjelmar (1996) for MSW incineration residues. Minor elements (100–1,000 mg/kg; 0.01 – 0.1 wt%) include Ba, Cd, Co, Cr, Cu, Mn, Sb, Sn and Sr. Trace elements (<100 mg/kg; < 0.01 wt%) comprise a broader list, with As, Mo, Ni and Se more frequently detected. Analytical techniques for APCr elemental characterisation include XRF, ICP-AES, ICP-OES and ICP-MS. Additionally, Bogush et al. (2015; 2019) used SEM-EDS to investigate the elemental composition of specific microstructural morphologies within loose powder samples, yielding semiquantitative results. However, a refined sample preparation protocol is required for SEM-EDS to deliver quantitative analysis of the entire APCr matrix. Such development would position SEM-EDS as a complementary, confirmatory tecnique, facilitating accurate correlation between APCr bulk composition and individual microstructures within a single analytical workflow.

Mineralogical analyses of UK APCr have predominantly been qualitative, identifying dominant phases without reporting concentrations beyond broad major/minor classification, as shown in Table 1. Common major phases include anhydrite ($CaSO_4$), calcite ($CaCO_3$), calcium hydroxychloride (CaOHCl), portlandite ($Ca(OH)_2$), halite (NaCl), sylvite (KCl) and quartz ($SiO_2$). Among these, CaOHCl, NaCl and KCl influence APCr leaching behaviour, whereas the more stable $CaCO_3$ and $Ca(OH)_2$ underpin carbon-capture treatments. The most complete UK APCr study, Bogush et al. (2015), extended the mineral phase inventory and confirmed identifications with complementary techniques, but still did not provide quantitative phase abundancies. Quantitative mineralogy is essential because phase abundance governs leachability, contaminant retention, and treatment reactivity. Without this information, it is difficult to predict leaching under disposal or reuse scenarios, assess regulatory compliance, or optimise processes like carbonation and washing. To enhance understanding of UK APCr behaviour, particularly leaching potential and treatment response, further research should identify additional phases, quantify individual phases with high precision and estimate the total crystalline and amorphous fractions.

APCr contains an organic fraction, typically measured as TOC, comprising trace organics, primarily polychlorinated dibenzo-p-dioxins and dibenzofurans, produced during waste incineration (Wiles, 1996). These dioxins and furans are Persistent Organic Pollutants (POPs) due to environmental persistence, resistance to degradation and bioaccumulation potential. In the UK, Robinson et. al (2004) remains the only report addressing organics in APCr. Their screening identified chlorinated aliphatic and aromatic hydrocarbons as predominant organic compounds, with dioxins and furans collectively counting around 11–27 μg/kg detected in solid residues. These were not detected in leachates, where TOC averaged around 5 mg/L. To our knowledge, no UK-based study has reported TOC in APCr solids. Both TOC solids and DOC in leachates are WAC-regulated; therefore, reporting these values in the literature before screening individual organic compounds is essential for assessing environmental risk from APCr and its recycling potential.

While most studies in Table 1 jointly analysed elemental composition and mineralogy, the UK APCr leaching behaviour remains underexplored. Robinson et al. (2004) examined leachate quality, reporting soluble salts, heavy metals, and organic indicators, but did not assess APCr's full release potential within the regulatory framework. Gunning et al. (2011) and Lee et al. (1999) examined exclusively heavy metal leaching, and only Gunning et al. (2011) compared results with hazardous WAC limits. Their data showed that among regulated metals, Pb leaching exceeded the hazardous WAC threshold, whereas Zn, despite its high solid-phase concentrations, leached below its limit, suggesting that APCr's environmental risk is primarily associated with Pb release. A holistic leaching analysis is required, extending beyond heavy metals to include soluble salts (chlorides, sulphates, fluorides), TDS, DOC, pH and conductivity, alongside a robust compliance assessment against WAC thresholds.

Sample representativeness is a critical gap in UK APCr characterisation, particularly given the nationwide growth in APCr-generating facilities and rising output. Most studies in Table 1, analysed only one or a few samples. Two studies explicitly sampled EfW facilities in London, the rest did not report regional origins. Although such approaches satisfied specific research objectives, they cannot capture the full complexity and variability of APCr composition. Limited sampling increases the risk of capturing outliers that misrepresent the broader chemical profile, leading to inaccurate assessments of environmental implications and treatment feasibility. Robinson et al. (2004) and Bogush et al. (2015) demonstrated greater representativeness, since detailed APCr analysis was their core objective. In 2002, when Robinson's sampling occurred, 12 UK MSW incinerators were operating. By Bogush's publication year (2015), 32 UK EfW facilities were fully operational (Tolvik Consulting Ltd, 2016). Their sampling covered

**Table 1**
Analytical approaches and characterisation gaps in UK APCr studies.

| Reference | Purpose | Representativeness | | | Analytical parameters and techniques | Characterisation gaps regarding WAC-regulated parameters ** and/or analytical techniques |
|---|---|---|---|---|---|---|
| | | No. of samples | Sample origin | Coverage (%) * | | |
| Lee et al. (1999) | Sintering as APCr management | 1 | 1 MSW incinerator | N/A | Solid: elemental composition (XRF) Leaching test (National Rivers Authority (NRA) )Leachate: Heavy metal leaching (ICP-AES) | Solid residue and leachate analyses did not cover the full set of WAC-regulated parameters and lacked comparison against WAC thresholds. |
| Robinson et al. (2004) | Report on incineration residues composition and treatment (carbonation and acid neutralisation) | 3 (composite) | 3 UK MSW incinerators | 25 | Solid: loss on drying at 105°C and 450°CLeaching test (BS EN 12457-4:2002) Solid and leachate: sulphates, chlorides, total nitrogen, N-NH$_4$, total metals, cyanide, dioxins and furans (non-reported analytical techniques) and trace organic compounds (List 1 screening test ***)Also leachate: TOC, biological and chemical oxygen demands, DOC, pH, conductivity (non-reported analytical techniques) | Solid residue and leachate analyses did not cover the full set of WAC-regulated parameters and lacked comparison against WAC thresholds.Leachate analysis focused on its quality (contaminant concentrations in leachate) but did not assess APCr's leaching potential (contaminant leachable concentrations in the solid) . |
| Fernández Bertos et al. (2004a) | Effects of accelerated carbonation on APCr | 6 | 6 UK MSW incinerators | N/A | Solid: moisture content, particle size distribution (non-reported analytical techniques), bulk density (water pycnometer), pH (electrometry), mineralogy (XRD), microstructure (SEM)Leaching test (BS EN 12457:2002)Leachate: chlorides and sulphates (Ion chromatography), major and minor elements leaching (ICP-OES) | Mineralogical analysis was qualitative, targeting dominant mineral phases only.<br>Solid residue and leachate analyses did not cover the full set of WAC-regulated parameters and lacked comparison against WAC thresholds. |
| Sun et al. (2008) | APCr carbonation kinetics | 1 | 1 London EfW facility | N/A | Elemental composition (XRF) Mineralogy (XRD)Physical properties: moisture content, porosity, mean particle size, density, tortuosity, total pore area (non-reported analytical techniques) | Analyses were not designed to assess WAC compliance.<br>Mineralogical analysis was qualitative, targeting dominant mineral phases only. |
| Dimech et al. (2008) | Production of sintered materials from APCr blends | Non-specified | 1 London EfW facility | N/A | Elemental composition (XRF, ICP-AES)<br>Mineralogy (XRD)<br>LOI at 1,025°C (gravimetry) | Analyses were not designed to assess WAC compliance.<br>Mineralogical analysis qualitatively categorised phases as major or minor but did not provide quantitative data. |
| Gunning et al. (2011) | APCr valorisation via accelerated carbonation | 2 | 2 MSW incinerator | N/A | Solid: total regulated metal contents (XRF)Leaching test (BS EN 12457-2:2002)Leachate: regulated metals (ICP-OES) | Solid residue and leachate analyses did not cover the full set of WAC-regulated parameters. |
| Bogush et al. (2015) | Elemental and mineralogical characterisation of APCr | 8 | 6 UK EfW facilities | 19 | Bulk elements (ICP-OES)Trace elements (ICP-MS)Chloride and sulphate (Ion chromatography)Mineralogy (XRD, confirmed by FTIR and DTG) Microstructure (SEM with SEI and BEI)Elemental composition of microstructures (SEM-EDS) | Analyses were not designed to assess WAC compliance.<br>Mineralogical analysis was strictly qualitative.<br>Elemental analysis of microstructures via SEM-EDS was semi-quantitative because measurements were taken on flat surfaces instead of polished sections. |
| Araizi et al. (2016) | Ultrasound-enhanced accelerated carbonation of APCr | 1 | 1 UK EfW facility | 3 | Elemental composition (XRF) Mineralogy (XRD)Particle size distribution (laser diffraction)Microstructure (SEM with SEI) | Analyses were not designed to assess WAC compliance.<br>Mineralogical analysis was qualitative, targeting dominant mineral phases only. |
| Bogush et al. (2019) | Changes in APCr composition due to water washing | 1 (composite) | 1 UK EfW facility | 2 | Particle size distribution (laser diffraction)Bulk elements (XRF and ICP-OES)Trace elements (ICP-MS)Mineralogy (XRD, confirmed by STA)Microstructure (SEM with SEI and BEI)Elemental composition of microstructures (SEM-EDS) | Analyses were not designed to assess WAC compliance.<br>Mineralogical analysis qualitatively categorised phases as major or minor but did not provide quantitative data.<br>Elemental analysis of microstructures via SEM-EDS was semi-quantitative because measurements were taken on flat surfaces instead of polished sections. |

* Coverage (%) = (number of sampled EfW facilities / number of fully operational EfW facilities) x 100, as detailed below:
Number of fully operational UK EfW facilities by 2002, the sampling period of Robinson et al. (2004): 12 (as reported in that study).
For other studies, sampling periods were not specified; therefore, Number of fully operational UK EfW facilities was considered based on publication year: 25: 2011 (Statista, 2025); 32: 2015; 37: 2016; 48: 2019 (Tolvik Consulting Ltd, 2016, 2017, 2021).
N/A: Data on the number of fully operational facilities was unavailable for calculation.
** WAC-regulated parameters: LOI and TOC in the solid matrix; heavy metals (As, Ba, Cd, Cr, Cu, Hg, Mo, Ni, Pb, Sb, Se and Zn), soluble salts (chlorides, sulphates and fluorides), TDS and DOC in the leachate.
*** List 1 trace organics in solid residues: chlorinated aliphatics and aromatics. List 1 trace organics in leachates: aromatic carboxylic acids, ketones, aldehydes, alcohols and esters.

approximately 25% and 19% of active sites, respectively, reasonable for characterisation at those times. However, APCr production increased from 80,000 tonnes in 2002 (Robinson et al., 2004) to 282,000 tonnes in 2015 (Tolvik Consulting Ltd, 2016), a 3.5-fold increase that required broader sampling. By end-2023, the UK had 60 operational EfW facilities, with APCr production estimated around 483,600 tonnes annually (Tolvik Consulting Ltd, 2024). This continued growth demands larger sample sets, regional origin reporting and updated characterisation frameworks to reflect current volumes, site diversity and evolving waste incineration processes and APC configurations across the country, to capture the full complexity and variability of APCr composition under current UK operational contexts.

APCr characteristics depend on MSW composition, incinerator operating conditions and APC technologies. Establishing relationships among these factors and APCr properties requires a stratified sampling approach within a monitoring programme aligned to operational variability to assess temporal effects and correlations with waste inputs and process parameters. However, previous research shows that linking APC systems to APCr properties is challenging due to high intra- and inter-system variability, particularly in elemental and mineral phase concentrations. Bodénan and Deniard (2003) reported strong convergence in mineral phase chemstry across diverse European MSW incinerators despite differing APC systems. Similarly, Bogush et al. (2015) ound APCr overall composition broadly consistent across facilities, though it may vary over time within each faciliity. Currently, diverse UK APCr streams are commonly mixed at facilities handling complex waste before stabilisation and disposal, with treatment decisions driven by WAC compliance rather than waste origin. Under these conditions, a management-oriented characterisation is more appropriate, focusing on residue composition, environmental properties and implications for downstream interventions (stabilisation, disposal, recycling). A sampling strategy targeting representative streams at a hazardous waste handling site, independent of upstream operational conditions, provides a broader dataset that captures variability and offers more representative coverage accros EfW facilities. This approach better informs regulatory compliance, treatment feasibility, and environmental safety for disposal or valorisation pathways.

## 2. Methodology

### 2.1. APCr sampling and sub-sampling

APCr samples were provided by Augean, a UK-based company specialist in managing hard-to-handle waste, including APCr from EfW plants primarily treating MSW (Augean, 2024). By 2020, Augean's received approximately 125,000 tonnes of APCr from at least 30 EfW sites across the UK, with per-facility inputs ranging from 7 to 24,000 tonnes. A sampling programme was designed to maximise coverage of APCr producers and regional origins, enabling characterisation of diverse streams from a management-oriented perspective, independent of upstream operational parameters. The design supports the study aim of evaluating composition, leaching behaviour and WAC compliance, to inform treatment and disposal strategies, focusing on residue properties rather than source-specific variables. This approach reflects real-world practice, where APCr management does not rely on the originating systems as different streams are routinely mixed at facilities handling complex waste prior to stabilisation and landfilling. Sampling occurred in two periods: November 2019 to March 2020, yielding 32 samples from 18 sites; and August to September 2020, yielding 10 samples from 4 sites. In total, 42 APCr samples were collected from 22 EfW plants across the UK, with sample masses proportional to the corresponding Augean input and averaging of 667 g. For traceability, samples were coded from APCr-01 to APCr-42 in order of collection, followed by a suffix indicating the sampling point P, uniquely associated with its corresponding geographical region. The regional distribution, shown in the supplementary information file attached to this paper, was as follows: South of Scotland (6 samples from P01 and P02), North Wales (8 samples from P03), South Wales (3 samples from P04 and P05), North East of England (4 samples from P06, P07, P08 and P09), Yorkshire and The Humber (1 sample from P10), West Midlands (6 samples from P11, P12 and P13), East Midlands (1 sample from P14), East of England (5 samples from P15 and P16), South West of England (6 samples from P17, P18 and P19), South East of England (2 samples from P20 and P21) and London (1 samples from P22). This sampling strategy provided substantially broader geographical coverage compared to previous studies, ensuring a more representative characterisation of APCr across the UK. Since 81% of the samples were collected in 2020, a year when APCr production was estimated at 450,000 tonnes and 54 EfW sites were fully operational (Tolvik Consulting Ltd, 2021), this cross-site sampling significantly enhanced representativeness, increasing coverage from 25% in previous studies to around 40% of UK EfW facilities.

The samples ranged in colour from dark grey to light beige and varied in physical form. Most were fine or granular powders, while some appeared as dry or wet lumps that disintegrated under slight pressure. Their solid, liquid or sludge consistency reflected the APCr technology (dry, semi-dry or wet) employed during flue gas cleaning. Particles of unburnt carbon from the original waste and activated carbon added during gas cleaning were observed. Some samples were odourless, while others emitted a strong odour, resulting from ammonia added during acid gas neutralisation. Sub-samples (200 g) were collected by coning and quartering (BS 3406-1:1986), dried at 105°C for 24 hr (BS EN 15934:2012) and stored in airtight plastic tubes for further characterisation.

### 2.2. Elemental analysis, microstructure and local elemental composition

Pressed-polished samples for elemental analysis using Scanning Electron Microscopy with Energy Dispersive X-ray Spectroscopy (SEM-EDS) were prepared by pressing approximately 2 g of dried APCr into a pellet, mounted in a rubber cup and covered with a mix of bisphenol-A based epoxy resin and cycloaliphatic polyamine hardener (2:1 ratio). Vacuum impregnation was performed in a KemVac unit at 100 mm Hg inverse pressure for 12 h. The cured resin-embedded sample was manually polished against silicon carbide grinding paper (grit 320) until exposing the surface, followed by fine polishing with oily-based diamond suspensions on a velvet pad in a Forcipol 102 modular system. This method preserves the native surface ensuring that elemental analysis remains quantitative and representative of the sample's true composition. It also avoids chemical etching, which can significantly alter the near-surface composition analysed by the electron-excited X-rays (Newbury and Ritchie, 2013). Loose powder samples for microstructural and local elemental analysis using SEM were prepared by pressing a stub with double-sided carbon conductive tape into APCr powder, ensuring particle adhesion. These samples were used to examine topography, morphology and particle size, and enabled qualitative and semi-quantitative analysis of local elemental composition of distinct structures within the waste matrix. Non-conductive specimens tend to accumulate negative charge under normal accelerated voltages, particularly above 10 kV (Heu, et al., 2019). To prevent charging under the electron beam, pressed-polished and loose powder samples were coated using an Agar Auto Carbon coater, which applied a transparent conductive layer (around 10 nm) via controlled carbon evaporation. Carbon was selected over metal sputtering because it provides conductivity without introducing grain-size artefacts that compromise high-magnification SEM imaging. Its low atomic number and transparency to electrons and soft X-rays (low-energy, long-wavelength X-rays) enable accurate Backscatter Electron Imaging (BEI) imaging and EDS analysis of light elements such as oxygen, a major APCr constituent. In contrast, Au coatings (typically 5–10 nm) form grains (10–12 nm), which become visible above 5,000X magnification, obscuring fine structural details. Furthermore, metals like Au, Pt or Cr absorb low-energy X-rays and cause spectral interferences (e.g., Cr overlaps with O), reducing microanalysis accuracy (Heu, et al., 2019). Although carbon layers are generally thicker than metal coatings, their impact on light-element detection is minimal, making ultrathin metal coatings unnecessary. Coated samples were stored in a desiccator containing silica gel crystals at relative humidity below 10%. Elemental composition, microstructure and local elemental composition analyses were conducted using a JSM-6460LV (JEOL) Scanning Electron Microscope at 8 mm working distance and 20 kV accelerating voltage. For elemental and local elemental composition, it was used an Xplore EDS detector (Oxford Instruments) targeting 25 elements: Al, As, Ba, Ca, Cd, Cl, Co, Cr, Cu, F, Fe, K, Mg, Mn, Mo, N, Na, Ni, O, P, Pb, S, Sb, Si, Zn. Calibration was performed using a certified Cobalt standard. Spectral data were acquired using AZtecLive software (Oxford Instruments NanoAnalysis, 2022). For microstructure analysis, Secondary Electron Imaging (SEI) and BEI detectors were employed at different magnifications.

### 2.3. Total metals contents

The WAC specify maximum leachable concentrations for 12 metals in solid waste: As, Ba, Cd, Cr, Cu, Hg, Mo, Ni, Pb, Sb, Se and Zn. Total metal contents indicate the maximum concentrations potentially available for long-term leaching. For analysis, 50 g of dried APCr was weighed into a digest vial and extracted with Aqua Regia (3 parts 35% HCl, 1 part 65% $HNO_3$) on a hot plate for 2–4 h (BS EN 13657:2002), oxidising organics and dissolving minerals. The liquid extract was diluted and analysed by Inductively Coupled Plasma – Optical Emission Spectrometry (ICP-OES) to quantify total metal concentrations.

### 2.4. Mineral characterisation

For X-Ray Diffraction (XRD) analysis, approximately 1 g of dried, ground APCr was mounted on an aluminium holder. Diffraction patterns were acquired using a Rigaku MiniFlex benchtop X-Ray diffractometer equipped with a Cu k-α X-ray tube, operating at 40 kV and 15 mA, and scanning 3°–70° 2θ at 0.015° steps and 2°/min. Mineral phases were identified using Rigaku PDXL software (Rigaku Corporation, 2021) and Crystallographic Information Files (CIF) from the Crystallography Open Database (Crystallography Open Database, 2021; Grazulis et al., 2009). For quantification, samples were spiked with 30% of rutile $TiO_2$ (internal standard) and analysed following the same procedure. Phase quantification was performed by Rietveld refinement in PDXL. Refinement quality was validated using the weighted profile R-factor ($R_{wp}$), which quantifies discrepancies between observed and calculated intensities while considering the statistical uncertainty of each data point in the diffraction pattern. $R_{wp}$ values ranged from 4% to 6% for most samples and increased to 7–8% in more complex cases, such as those with numerous mineral phases or diffraction patterns exhibiting significant background deformations. These ranges indicate a good level of agreement, since $R_{wp}$ values below 10% are generally considered acceptable for Rietveld refinements, with lower values reflecting a closer fit between observed and calculated profiles.

### 2.5. Organic matter indicators

Loss on Ignition (LOI) estimates organic matter content by measuring mass loss after thermal treatment. For this analysis, 20 g of dry APCr was fired in a muffle furnace at 550°C for 4 h (BS EN 15935:2021). LOI was calculated as the percentage of weight loss resulting from combustion. Total organic carbon (TOC) quantifies carbon oxidised to $CO_2$ during combustion, excluding inorganic carbon removed during acid pretreatment. For TOC analysis, APCr was treated with 85% phosphoric acid at 40°C to eliminate inorganic carbon (BS EN 13137:2001). After evaporating excess acid, the sample was analysed using a TOC analyser with a Non-Dispersive Infrared Detector (TOC-NDIR). Combustion occurred at 1,600°C in an induction furnace with oxygen as the carrier gas. TOC was calculated as a percentage of the original sample mass.

### 2.6. Leaching tests

Leaching tests were conducted to quantify the transfer of soluble substances from APCr to water over an extended period, following the granular waste compliance leaching test (BS EN 12457-2:2002). For analysis, 90 g of dried, ground APCr ($<$4 mm) was extracted for 24 h with 900 mL of deionised water in a polyethylene plastic bottle using a Hedolph Reax 20 overhead shaker. The liquid fraction (leachate) was filtered through a 0.45 μm membrane using vacuum filtration, and immediately tested for TDS, pH and conductivity using potentiometric techniques. It was then analysed for metals by ICP-OES, for chlorides, fluorides and sulphates by Ion Chromatography and for DOC by TOC-NDIR. Results were contrasted against WAC limits for hazardous waste acceptance at landfills, calculated at 10 L/kg total release (European Union, 2003).

## 3. Results and discussion

### 3.1. Elemental composition

Fig. 1A illustrates the elemental profiles of 41 APCr samples, showing the concentration distribution of 17 elements detected (out of 25 targeted by SEM-EDS), normalised to 100%. O, Ca and Cl consistently dominate the composition, collectively exceeding 80 wt% in most samples. O and Ca are mainly derived from alkaline reagents used in flue gas neutralisation, including hydrated lime ($Ca(OH)_2$), quick lime (CaO) and limestone ($CaCO_3$ in calcite and aragonite forms). Additional oxygen can originate from sodium hydroxide (NaOH) and sodium bicarbonate ($NaHCO_3$), which are employed to a lesser extent for acid gas neutralisation. Samples APCr-05-P01 from South Scotland and APCr-03-P03, APCr-11-P03 and APCr-18-P03 from North Wales exhibited profiles markedly different from the rest of the batch. These samples showed O concentrations above 73 wt%, indicating substantially higher levels of oxides, hydroxides, sulphates and carbonates, likely formed through neutralisation reactions or from residual unreacted reagents. Cl abundance reflects its origin in MSW, especially from the synthetic plastic polyvinyl chloride (PVC ($(C_2H_3Cl)_n$), cleaning agents, and salt-rich food waste. During incineration, Cl volatilises as HCl, which is neutralised by alkaline reagents to form chlorides such as $CaCl_2$, NaCl, and KCl. In addition, Cl levels can be associated with the interactions between Si, Al rich compounds with alkali metals (Na and K). Si and Al in the APCr samples originate from the MSW inorganic fraction, particularly glass, ceramics and soil. These thermally stable elements persist through incineration and contribute to the formation of refractory mineral phases such as quartz and aluminosilicates. In contrast, Na and K, derive

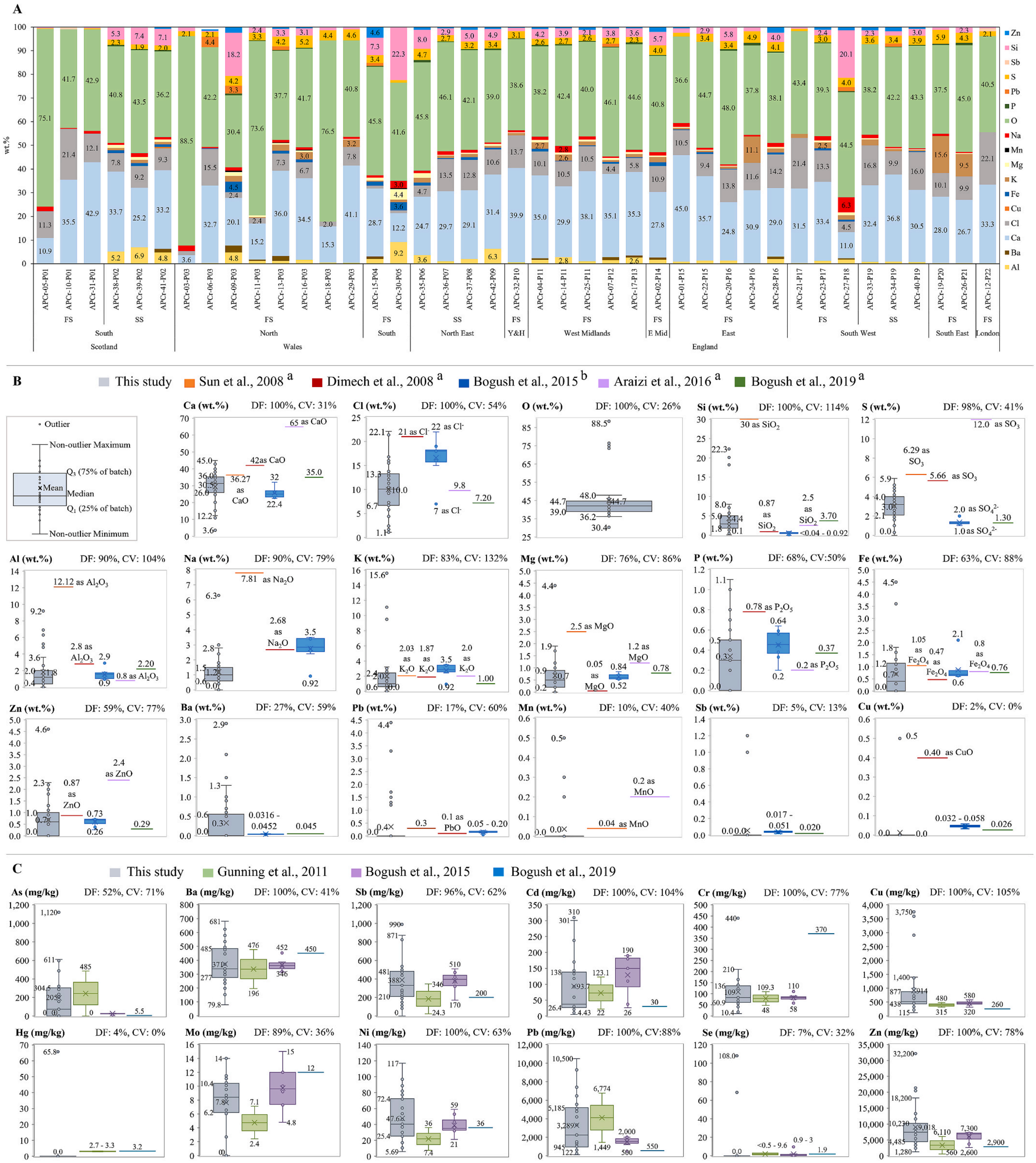

**Fig. 1. Elemental composition of UK APCr.** A: SEM-EDS profiles of APCr samples. England's regional labels are abbreviated as follows: 'Y&H' for Yorkshire and The Humber, 'E Mid' for East Midlands; other region names are shown in full. B: Variability in SEM-EDS elemental analysis compared with other UK studies. C: Variability of total metal contents analysed by ICP-OES, compared with other UK studies. DF (Detection Frequency) = % of samples in which each element was detected. CV (Coefficient of Variation) = (Standard Deviation x 100) / Mean. SEM-EDS detection limits (wt.%): F (0.5), Mo (0.3), N (3.7), O (0.2), Pb (0.2), Sb (0.2), others (0.1). SEM-EDS data were unavailable in the referenced studies. Comparative techniques include [a]XRF and [b]ICP-OES, ICP-MS, IC for Cl as Cl$^-$ and S as $SO_4^{2-}$. ICP-OES detection limits (mg/kg): As (4.04), Ba (0.231), Cd (0.219), Cr (0.325), Cu (0.917), Hg (0.972), Mo (2.39), Ni (0.260), Pb (0.548), Sb (4.44), Se (1.77), and Zn (7.68). Concentrations below detection limits are represented as 0.0 in boxplot labels.

from food residues, detergents, biomass, and flue gas treatment additives like $NaHCO_3$, and tend to be more soluble and mobile. During waste incineration and flue gas treatment, they form both soluble salts and stable aluminosilicate phases. Na and K were present in most samples, though their concentrations varied without a consistent pattern. Notably, the samples APCr-09-P03 and APCr-30-P05 from North and South Wales, respectively, and APCr-27-P18 from South of England, showed elevated Si content (around 20 wt%) but lower Cl concentrations (<5 wt%). According to Roberts, et al. (2019), aluminosilicates added during high-K, high-Cl biomass combustion promote the formation of stable, high-melting-point compounds that bind K, while Cl is released as HCl. A similar mechanism occurs during MSW incineration, where aluminosilicates react with alkali chlorides, immobilising K and Na and releasing Cl as HCl, thereby reducing Cl content in the resulting APCr.

S was consistently detected in most APCr samples, although at low concentrations (<below 6 mg/kg). Among the samples from the first point in South Scotland, S was present in APCr-05-P01 and APCr-31-P01 at just detectable concentrations, while it was not detected in APCr-10-P01.This element in MWS typically originates from plastics, textiles, and batteries. Its low abundance or absence in APCr, may indicate effective waste segregation, since residues such as textiles and batteries should not enter the incineration feed. When present, S remaining in the waste oxidises to $SO_2$ during combustion and is subsequently captured via flue gas neutralisation, forming sulphates like $CaSO_4$, associated to APCr leaching.

Similarly, elements detected infrequently and at concentrations near the SEM-EDS detection limits (as specified in Fig. 1 caption), reflect the heterogenous composition of MWS. These include Pb and Ni/Ca from sealed batteries, Cu and As from preserved food, and Sb from flame-retardant materials. Such trace constituents may become incorporated into mineral phases during incineration.

Several samples collected from the same facility at different times exhibited similar elemental profiles. For instance, samples −P02 from South Scotland, contained essentially the same elements at comparable concentrations. Similarly, samples −P19 from South West of England showed very similar profiles, with only slight differences in K content. In contrast, other samples differed markedly. The −P03 group from North Wales displayed the greatest variation in major element concentrations, with O ranging from 30.4 to 88.5 mg/kg, Ca from 3.6 to 41.1 mg/kg, Cl from 1.7 to 15.5 mg/kg and Si from 0.4 to 18.2 mg/kg, as well presence or absence of elements such as Fe. Likewise, samples −P17 from South West of England, although comparable in major element concentrations, differed in the number of elements detected. This variability, previously noted in international and UK APCr studies (Quina et al., 2008; Bogush et al., 2015), reflects temporal shifts in MSW composition and incineration or APC system operations. Furthermore, APCr samples from the same region but different EfW facilities showed notable differences. For example, in South Scotland, the −P01 group contained fewer elements and higher concentrations of O and Cl compared to the −P02 group. Similarly, samples APCr-15-P04 and APCr-30-P05 from South Wales showed marked differences in concentration of most elemental concentration. Conversely, some samples from different EfW facilities within the same region exhibited similar elemental profiles, such as APCr-36-P07 and APCr-37-P08 from North East England or APCr-19-P20 and APCr-26-P21from South East England. Overall, no consistent intra- or interregional trends emerged in qualitative or quantitative elemental profiles, highlighting the dynamic nature of APCr generation across EfW facilities and within individual facilities over time.

Fig. 1B presents the concentration variability of chemical elements detected in APCr samples, alongside comparative data from previous UK studies. Although the detection limit was 0.1 wt% for most elements, classification as major components (>0.1 wt%) considered both concentration and detection frequency, defined as the percentage of samples in which each element was detected. Major elements included Ca, Cl, O and Si (detected in all samples) and Al, Fe, K, Mg, Na, P, S, Zn (detected in at least 59% of samples). O and Ca showed the highest concentrations (30.4–88.5 wt% and 3.6–45 wt%, respectively) and the lowest variability, with coefficients of variation (CVs) of 26% and 31%, respectively. In contrast, Al, K and Si exhibited markedly higher variability, with CVs approaching or exceeding 100%, and outliers well above the interquartile ranges. This variability likely reflects differences in MSW composition, incineration conditions and APC systems across EfW facilities.

Ba, Mn, Pb, Sb and Cu were detected in fewer samples, with Ba being the most frequent, present in up to 27% of the batch. Boxplots for these elements show concentrations typically below 0.1 wt%, though outliers, particularly for Pb, evidence that levels can occasionally become major, raising environmental and regulatory concerns. In contrast, As, Cd, Co, Cr, F, Mo, N and Ni were not detected in any sample, despite their known occurrence in APCr. Further analysis using techniques with lower detection limits is recommended, particularly for trace metals linked to leaching.

Overall, the elemental composition of APCr observed in this study closely aligns with previous findings. For frequently detected elements, concentrations reported in the literature generally fell within the interquartile ranges defined in this work. Ca and Na concentrations were particularly consistent with the high non-outlier values estimated in this study, reflecting their origin in both waste feedstock and flue gas treatment reagents. For less frequently detected elements (Ba, Mn, Pb, Sb and Cu), agreement between outlier values and those reported in other studies, supports the need for complementary techniques to quantifying trace and minor constituents. The concentrations of S and Ca reported by Araizi et al. (2016) and Al, Na, S and Si by Sun et al., (2008) were significantly higher than those found in this and other referenced works, suggesting that both studies likely analysed atypical samples. These anomalies may reflect abundance outliers, highlighting the importance of assessing representative APCr batches, as done in this work, rather than relying on single-sample evaluations, to ensure robust and generalisable compositional insights.

### 3.2. Total metal contents

Fig. 1C summarises the total contents of 12 WAC-regulated metals in 27 APCr samples analysed by ICP-OES, alongside comparative data from recent UK studies. Zn was present in all samples at major levels (>1,000 mg/kg), while Cu and Pb appeared at minor to major levels (>100 mg/kg), and Ba, Cd, Cr and Ni were found at trace to minor levels (<1,000 mg/kg), and most samples contained trace to minor concentrations of As and Sb, and trace levels (<100) of Mo. The relatively low concentrations of Cd, Cr, and Ni, and near absence of Hg in the APCr samples, likely reflect their declining use in consumer goods, prompted by toxicity concerns and regulatory restrictions under RoHS (Restriction of Hazardous Substances) and REACH (Registration, Evaluation, Authorisation and Restriction of Chemicals). In contrast, the prevalence of Pb suggests its persistent use in certain products, despite being similarly regulated. The rareness of Hg in APCr is also consistent with its volatilisation during MSW incineration, where it reacts with HCl in flue gases to form $HgCl_2$, a highly soluble compound removed in the water spray tower (Song et al., 2004).

Substantial variability in total metal contents was observed across APCr samples, with CVs ranging from 36% to 105% for consistently detected metals, and from 0% to 32% for infrequently detected Se and Hg. This aligns with the heterogeneity in elemental composition observed by SEM-EDS, and reflects differences in MSW input, incineration conditions and APC systems across EfW facilities. Metal concentrations broadly encompassed those reported in previous UK research, with interquartile ranges often overlapping published averages, particularly Bogush et al. (2015). However, boxplot inner points reveal that As, Cu, Ni, Pb and Zn, were generally present at higher concentrations than those previously reported. Notably, when detected, Hg and Se concentrations exceeded previous reports by one and two orders of magnitude, respectively. These elevated levels likely reflect atypical samples, supported by their low detection frequencies, 4% for Hg and 7% for Se.

## *3.3. Mineralogy*

### *3.3.1. Identification and quantification of mineral phases*

Fig. 2 summarises the qualitative and quantitative mineralogical composition of 42 APCr samples, alongside comparative data from prior UK-based studies. Seven phases were defined as major, based on high detection frequencies (55–88%) and substantial mean concentrations (4.10–17.3 wt%): $CaCO_3$, $CaSO_4$, $Ca(OH)_2$, CaOHCl, NaCl, KCl and $SiO_2$. This aligns with the referenced UK studies and with well-known APCr mineralogy. APCr are highly reactive to $CO_2$ because of elevated calcium hydroxide content, particularly $Ca(OH)_2$ and CaOHCl (Costa, 2009; Baciocchi et al., 2009). $CaCO_3$, the most frequently detected phase, also plays a key role in $CO_2$ capture. This reactivity has been exploited in UK studies for APCr valorisation and stabilisation via carbonation treatments (Araizi et al., 2016; Gunning et al., 2011; Sun et al., 2008). Conversely, high concentrations of Cl-bearing salts (CaOHCl, NaCl and KCl), and $CaSO_4$ are strongly associated with elevated leaching of soluble species. To mitigate these effects, water washing and stabilisation/solidification treatments are commonly applied, improving APCr performance in reuse and disposal scenarios. Interestingly, CaOHCl, the most abundant phase (1.5–43.5 wt%), plays a dual role in APCr chemistry (reactivity with $CO_2$ and leaching risk) due to its hydroxide and chloride components.

A total of 45 distinct mineral phases, including 21 not previously reported in APCr, were detected across the analysed samples, positioning this study as the most comprehensive mineralogical characterisation of APCr to date. This significantly expands the known APCr mineral profile compared to prior investigations across Asia and Europe (Alba et al., 1997; Abbas et al., 2003; Araizi et al., 2016; Atanes et al., 2019; Bodénan and Deniard, 2003; Bogush et al., 2015; Cao et al., 2021; Chen et al., 2012; Chimenos et al., 2005; Dimech et al., 2008; Dontriros et al., 2020; Fan et al., 2022; Fernández Bertos et al., 2004b; Geysen et al., 2004; Han et al., 2022; He et al., 2004; Hu, 2005; Karlfeldt Fedje et al., 2010; Keppert et al., 2015; Li et al., 2004; Li et al., 2017; Nikravan et al., 2020; Quina et al., 2008; Sun et al., 2008; Yang et al., 2017). The most detailed previous study, focused on UK APCr, reported 21 mineral phases (Bogush et al., 2015), while studies in China identified 12 (He et al., 2004) and more recently, 11 (Fan et al., 2022). Several newly identified phases are Si-enriched, likely derived from Si-bearing waste (e.g. glass, ceramics) and silicate-based flue gas treatment additives. Notable examples include clinotobermorite ($Ca_5H_8O_{21}Si_6$) in 26% of samples, kumdykolite ($NaAlSi_3O_8$) in 17%, and larnite ($Ca_2SiO_4$) and sanidine ($KAlSi_3O_8$), each in 12%. In some samples, Si-bearing phases contributed substantially to the mineral fraction. For instance, APCr-32-P10 from Yorkshire and The Humber, which exhibited the highest total mineral fraction (77 wt%), contained 17 wt% of clinotobermorite and 22 wt% of larnite, making it a particularly interesting stream for further evaluation. Si-bearing phases, along with major $SiO_2$, may enhance APCr's chemical stability through carbonation treatment. Since $Ca(OH)_2$ carbonates to $CaCO_3$, the matrix densifies and brings silicates into closer contact with reactive calcium phases. Future work should assess whether existing Si-phases promote additional Ca-silicate-hydrates (C–S–H) and how this influences metal binding and mobility. Si-bearing phases also impart pozzolanic behaviour, previously investigated in APCr from other countries for cementing materials (Huang & Chu, 2003; Ghouleh & Shao, 2018; Ashraf et al., 2019) and supplementary cementitious materials (Keppert, et al., 2015; Dontriros et al., 2020). Similar evaluations are needed for UK-generated APCr.

Other commonly detected phases include bassanite ($CaSO_4{\cdot}0.5H_2O$) and magnesium oxide hydroxide ($Mg_3O_2(OH)_2$), each found in 24% of samples, and zincowoodwardite ($Al_{0.375}H_6O_{2.686}S_{0.188}Zn_{0.625}$) in 38%. The latter two, along with botallackite ($Cu_2(OH)_3Cl$), cerussite ($PbCO_3$) and tobermorite ($Ca_{2.25}H_{3.5}O_{10}Si_3$) have only been reported in UK APCr (Bogush et al., 2015). Based on their chemical structure, bassanite and

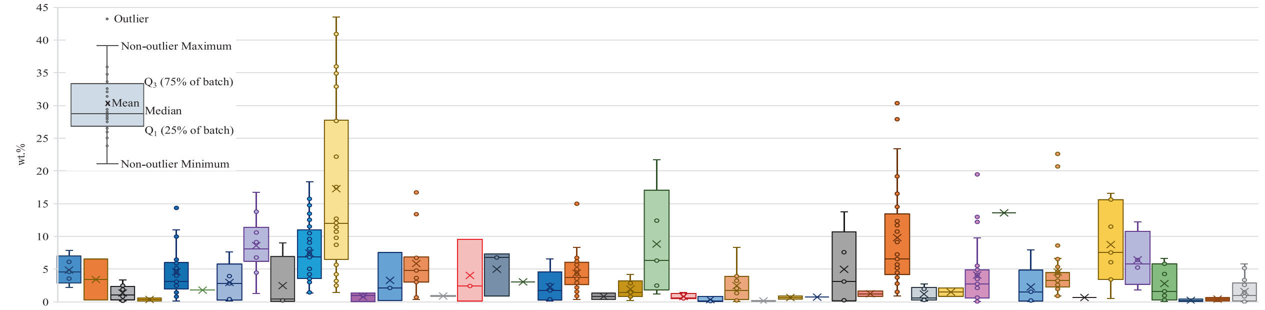

| | 1 | 2 | 3 | 4 | 5 | 6 | 7 | 8 | 9 | 10 | 11 | 12 | 13 | 14 | 15 |
|---|---|---|---|---|---|---|---|---|---|---|---|---|---|---|---|
| Max wt.% (including outliers) | 7.90 | 6.54 | 3.34 | 0.56 | 14.59 | 1.78 | 7.59 | 16.69 | 9.00 | 18.33 | 43.48 | 1.37 | 7.52 | 16.71 | 0.97 |
| Min wt.% (including outliers) | 2.21 | 0.30 | 0.13 | 0.14 | 0.13 | 1.78 | 0.11 | 1.26 | 0.02 | 1.34 | 1.48 | 0.01 | 0.19 | 0.37 | 0.82 |
| Average | 4.87 | 3.42 | 1.37 | 0.35 | 4.59 | 1.78 | 2.97 | 8.61 | 2.46 | 7.46 | 17.29 | 0.77 | 3.28 | 5.85 | 0.90 |
| CV% | 45 | 129 | 82 | 84 | 85 | 0 | 102 | 51 | 177 | 60 | 74 | 90 | 116 | 86 | 11 |
| Detection frequency % | 12 | 5 | 19 | 5 | 62 | 2 | 12 | 24 | 10 | 88 | 67 | 7 | 7 | 26 | 5 |
| First time reported in APCr | ✓ | ✓ | ✓ | ✓ | | | | | | | | | ✓ | ✓ | ✓ |
| Fernández Bertos et al. (2004) | | | | | X | | | | | X | | | | | |
| Sun et al. (2008) | | | | | X | | | | | X | X | | | | |
| Dimech et al. (2008) | | | | | X | | | | | X | X | | | | |
| Bogush et al. (2015) | | | | | X | | | | O | X | X | O | | | |
| Araizi et al. (2016) | | | | | X | | | | | X | X | | | | |
| Bogush et al. (2019) | | | | | X | | | | | X | X | | | | |

| | 16 | 17 | 18 | 19 | 20 | 21 | 22 | 23 | 24 | 25 | 26 | 27 | 28 | 29 | 30 |
|---|---|---|---|---|---|---|---|---|---|---|---|---|---|---|---|
| Max wt.% (including outliers) | 9.55 | 7.31 | 3.05 | 6.56 | 14.99 | 1.31 | 4.20 | 21.73 | 1.45 | 0.82 | 8.34 | 0.21 | 0.90 | 0.72 | 13.79 |
| Min wt.% (including outliers) | 0.11 | 0.87 | 3.05 | 0.12 | 0.38 | 0.36 | 0.20 | 1.20 | 0.44 | 0.07 | 0.01 | 0.07 | 0.41 | 0.72 | 0.10 |
| Average | 4.03 | 4.99 | 3.05 | 2.28 | 4.39 | 0.84 | 1.96 | 8.82 | 0.82 | 0.33 | 2.48 | 0.14 | 0.65 | 0.72 | 4.96 |
| CV% | 122 | 72 | 0 | 114 | 63 | 80 | 75 | 96 | 54 | 126 | 102 | 68 | 53 | 0 | 117 |
| Detection frequency % | 7 | 7 | 2 | 12 | 76 | 5 | 17 | 12 | 12 | 7 | 24 | 5 | 5 | 2 | 12 |
| First time reported in APCr | ✓ | | ✓ | | | | ✓ | ✓ | | | | ✓ | ✓ | | ✓ |
| Fernández Bertos et al. (2004) | | X | | | X | | | | | | | | | | |
| Sun et al. (2008) | | | | | | | | | X | | | | | X | |
| Dimech et al. (2008) | | | | | X | | | | | | | | | | |
| Bogush et al. (2015) | | X | | | X | | | | X | | O | | | | |
| Araizi et al. (2016) | | | | | X | | | | X | | | | | | |
| Bogush et al. (2019) | | X | | | X | | | | X | | | | | | |

| | 31 | 32 | 33 | 34 | 35 | 36 | 37 | 38 | 39 | 40 | 41 | 42 | 43 | 44 | 45 |
|---|---|---|---|---|---|---|---|---|---|---|---|---|---|---|---|
| Max wt.% (including outliers) | 1.64 | 30.36 | 2.71 | 2.13 | 19.46 | 13.60 | 7.94 | 22.62 | 0.66 | 16.55 | 12.24 | 6.61 | 0.42 | 0.71 | 5.82 |
| Min wt.% (including outliers) | 0.83 | 0.87 | 0.18 | 0.86 | 0.01 | 13.60 | 0.01 | 0.87 | 0.66 | 0.50 | 1.84 | 0.06 | 0.04 | 0.08 | 0.01 |
| Average | 1.23 | 9.80 | 1.19 | 1.49 | 4.10 | 13.60 | 2.29 | 4.56 | 0.66 | 8.74 | 6.43 | 2.80 | 0.23 | 0.42 | 1.58 |
| CV% | 47 | 82 | 88 | 60 | 121 | 0 | 142 | 104 | 0 | 69 | 67 | 97 | 118 | 62 | 118 |
| Detection frequency % | 5 | 60 | 17 | 5 | 55 | 2 | 12 | 79 | 2 | 17 | 10 | 17 | 5 | 10 | 38 |
| First time reported in APCr | ✓ | | | ✓ | | ✓ | ✓ | | ✓ | | | ✓ | ✓ | | |
| Fernández Bertos et al. (2004) | | X | | | X | | | X | | | | | | | |
| Sun et al. (2008) | | X | | | X | | | X | | | | | | | |
| Dimech et al. (2008) | | X | | | | | | X | | | | | | | |
| Bogush et al. (2015) | | X | | | X | | | X | | O | | | | | O |
| Araizi et al. (2016) | | X | | | | | | | | | | | | | |
| Bogush et al. (2019) | | | | | X | | | X | | | | | | | |

1 Akermanite $Ca_2MgSi_2O_7$
2 Albite $NaAlSi_3O_8$
3 Anatase $TiO_2$
4 Anglesite $PbSO_4$
5 Anhydrite $CaSO_4$
6 Anorthite $CaAl_2Si_2O_8$
7 Arcanite $K_2SO_4$
8 Bassanite $CaSO_4{\cdot}0.5H_2O$
9 Bottalackite $Cu_2(OH)_3Cl$
10 Calcite $CaCO_3$
11 Calcium Hydroxychloride CaOHCl
12 Cerussite $PbCO_3$
13 Chlorapatite $Ca_5(PO_4)_3Cl$
14 Clinotobermorite $Ca_5H_8O_{21}Si_6$
15 Dipotassium oxide $K_2O$
16 Ettringite $Ca_6Al_2(SO_4)_3(OH)_{12}{\cdot}26H_2O$
17 Gehlenite $Ca_2Al(AlSiO_7)$
18 Grossite $CaAl_4O_7$
19 Gypsum $CaSO_4{\cdot}2H_2O$
20 Halite NaCl
21 Hematite $Fe_2O_3$
22 Kumdykolite $NaAlSi_3O_8$
23 Larnite $Ca_2SiO_4$
24 Lime CaO
25 Litharge PbO
26 Magnesium oxide hydroxide $Mg_3O_2(OH)_2$
27 Monteponite CdO
28 Nickel ferrite $NiFe_2O_4$
29 Periclase MgO
30 Perovskite $CaTiO_3$
31 Phosphorous pentoxide $P_2O_5$
32 Portlandite $Ca(OH)_2$
33 Potassium tetrachloro zincate $K_2ZnCl_4$
34 Pseudowollastonite $CaSiO_3$
35 Quartz $SiO_2$
36 Rutile $TiO_2$
37 Sanidine $KAlSi_3O_8$
38 Sylvite KCl
39 Tetrapotassium lead oxide $K_4PbO_4$
40 Tobermorite $Ca_{2.25}H_{3.5}O_{10}Si_3$
41 Whitlockite $Ca_3(PO_4)_2$
42 Zinc chloride $ZnCl_2$
43 Zinc oxysulphate $Zn_3O(SO_4)_2$
44 Zincite ZnO
45 Zincowoodwardite $Al_{0.375}H_6O_{2.686}S_{0.188}Zn_{0.625}$

**Fig. 2. Qualitative and quantitative characterisation of APCr mineralogy by XRD analysis.** Boxplots show the variability in mineral phase concentrations across samples, with coefficients of variation (CV%) indicating relative dispersion around mean values. ✓denotes phases newly identified in APCr and thus newly reported in UK APCr. X indicates phases previously reported in the UK literature. O denotes phases exclusively detected in UK APCr.

botallackite are likely contributors to leachable fractions, whereas magnesium oxide hydroxide, cerussite and tobermorite are more closely associated with stable fractions. Zincowoodwardite is a rare hydrated basic sulphate mineral belonging to the hydrotalcite group, with general formula $[Zn_{1\text{-}x}Al_x(OH)_2][(SO_4)_{x/2}(H_2O)_n]$ (Crystallography Open Database, 2021). Though solubility data are limited, its structure suggests low solubility under alkaline conditions typical of APCr, supporting its potential role in Zn immobilisation. Additional Zn-enriched phases included potassium tetrachloro zincate ($K_2ZnCl_4$), zinc chloride ($ZnCl_2$), zinc oxysulphate ($Zn_3O(SO_4)_2$) and zincite (ZnO). Other heavy metals were present in mineral forms: Pb in anglesite ($PbSO_4$), cerussite ($PbCO_3$), litharge (PbO) and tetrapotassium lead oxide ($K_4PbO_4$); Cd as Monteponite (CdO), and nickel as nickel ferrite ($NiFe_2O_4$).

Mineral phase concentrations in APCr showed substantial variability, with CVs ranging from 11% to 177% for phases detected in more than one sample. Among major phases, CVs typically fluctuated between 60% and 85%, but exceeded 100% for $Ca(OH)_2$, and KCl. CVs above 100% were particularly observed in phases detected in $\leq$ 12% of samples and in zincowoodwardite. This variability indicates inconsistent patterns, limiting the reliability of average concentration estimates for mineral phases in UK APCr. Nevertheless, the observed ranges support quantification of individual phases and estimation of total mineral fractions, enabling approximation of amorphous content. As discussed, APCr properties are influenced not only by dominant phases but also by those present at lower concentrations or with limited occurrence. The less frequent phases could exert significant influence, reinforcing the need to consider both major and minor constituents when evaluating APCr's environmental and technological properties. Such insights are critical for informing resource recovery, treatment, and recycling strategies.

### 3.3.2. *Estimation of the amorphous fraction and mineral phase distribution within samples*

Diffractograms of some APCr samples revealed amorphous material, indicated by background deformations (humps), mainly between 20° and 40° 2θ, and broadened peaks. For instance, Fig. 3A shows APCr-23-P17 with minimal amorphous content, as its background did not deform, while APCr-02-P14 and APCr-30-P05 exhibited humps around 30° and 27° 2θ, respectively. Amorphous content may be non-crystalline or poorly crystalline material (Bodénan and Deniard, 2003; Bogush et al., 2015) resulting from high-temperature chemical interactions during waste incineration. Non-crystalline materials lack long-range atomic order and include amorphous silica ($SiO_2{\cdot}nH_2O$) originated from Si-based waste, gas neutralisation additives and condensation byproducts, activated carbon from flue gas filtration, and amorphous metal oxides formed during incineration like $Fe_2O_3$, $Al_2O_3$ or $TiO_2$. Poorly crystalline materials exhibit short-range order and lack well-defined lattice structures, typical of transitional phases such as bassanite (from gypsum). Other examples include Ca-Si-hydrates, such as tobermorite and clinotobermorite, layered double hydroxides like zincowoodwardite, and magnesium oxide hydroxide. Given the limited characterisation of the amorphous phase, further systematic investigations are essential to determine its composition, hydration states, and environmental behaviour. To complement XRD, future research should incorporate complementary techniques to elucidate APCr's amorphous characteristics beyond total content. FTIR and Raman spectroscopy can reveal structural disorder and bonding environments associated with non-crystalline or poorly crystalline components. For example, Bogush et al. (2015) identified poorly crystalline aragonite in UK APCr through FTIR, whereas XRD failed to detectet this phase. Similarly, Bodénan and Deniard (2003) confirmed major mineral phases and identified the infrared signature of CaOHCl in APCr from European MSW incineration. Combined thermal analysis, including Differential Scanning Calorimetry (DSC) for glass transition detection and Thermogravimetric Analysis (TGA) for thermal stability and decomposition behaviour, can further enhance characterisation. For instance, Bodénan and Deniard (2003) using DSC/TGA and Bogush et al. (2015) usign TGA, identified four decomposition temperature ranges and identified peaks corresponding to $Ca(OH)_2$, $CaCO_3$ and CaOHCl. Advanced approaches, such as Pair Distribution Function (PDF) analysis and solid-state NMR can offer insights into short-range atomic arrangements.

Fig. 3B summarises the total mineral and amorphous contents, alongside the distribution of individual mineral phases across 42 APCr samples. Only APCr-04-P11 from West Midlands, APCr-06-P03 from North Wales and APCr-37-P08 from North East England (7% of the batch) exhibited statistically equivalent contents of crystalline and amorphous material, as indicated by confidence intervals overlapping the 50% mark. Among the remaining samples, approximately half were dominated by crystalline phases and half by amorphous content. Crystalline fractions ranged from 13.53 ± 0.58 wt% to 76.73 ± 1.99 wt%, whereas amorphous contents varied between 23.27 ± 1.99 wt% and 86.47 ± 0.58 wt%. Overall, the APCr samples contained approximately 10 wt% more amorphous material than crystalline. The regional analysis shows that APCr from South Scotland, North Wales, Yorkshire and The Humber, West Midlands, South West England, South East England and London contained proportions over 50% of crystalline contents. In contrast, APCr from South Wales, North East England, East Midlands and East of England were predominantly amorphous. Samples collected from the same EfW site at different times showed consistent trends, with all or most exhibiting either crystalline or amorphous dominance, such as the −P03 group from North Wales clearly demonstrating crystalline prevalence. This distinction is important for practice because APCr management and stabilisation strategies may need to differentiate protocols according to phase assemblage, given the differing stability, leaching behaviour and processing responses associated with amorphous against crystalline fractions.

The mineral phase distribution in APCr samples, shown in Fig. 3B, demonstrates the predominance of the seven major phases across the whole sample batch, with notable regional variability. CaOHCl stands out as the most abundant phase in most samples, followed by $CaCO_3$, $Ca(OH)_2$, and $CaSO_4$, particularly in samples from South Scotland and several English regions, including North East, East, South West and London. This trend persists irrespective of whether the total mineral fraction or amorphous fraction dominates. APCr from England exhibited higher enrichment in the three chloride-bearing phases (CaOHCl, NaCl and KCl), which frequently coexisted, although combined NaCl and KCl accounted for less than half the wt.% of CaOHCl. Furthermore, APCr from East, South West and South East of England, and London often lacked or contained minimal concentrations of $SiO_2$, a stable phase under environmental conditions. Collectively, these characteristics suggest that APCr from England may pose greater management challenges compared to APCr from Wales and South Scotland, which contained lower contents on leachable salts.

The mineralogy of APCr from Wales deserves particular attention due to its distinct composition and the greatest variability observed among all regions. The eight samples (−P03) collected from a single EfW facility in North Wales exhibited markedly heterogeneous profiles, with the highest numbers of crystalline phases (6 – 14). Noteworthy, phases included bassanite ($CaSO_4{\cdot}0.5H_2O$) and anhydrite ($CaSO_4$), occurring individually or together, as well as tobermorite ($Ca_{2.25}H_{3.5}O_{10}Si_3$) and calcite ($CaCO_3$), although no individual phase exhibited predominance. Similarly, samples from South Wales displayed diverse mineralogical profiles, but with a clear predominance of calcite ($CaCO_3$) and quartz ($SiO_2$). Despite the presence of soluble sulphates (bassanite and anhydrite) which may adversely affect the durability of newly developed materials, the occurrence of Si-based minerals including quartz ($SiO_2$), tobermorite ($Ca_{2.25}H_{3.5}O_{10}Si_3$), gehlenite ($Ca_2Al(AlSiO_7)$) and akermanite ($Ca_2MgSi_2O_7$), among others, suggests that APCr from Wales could serve as a promising feedstock for recycling into construction applications.

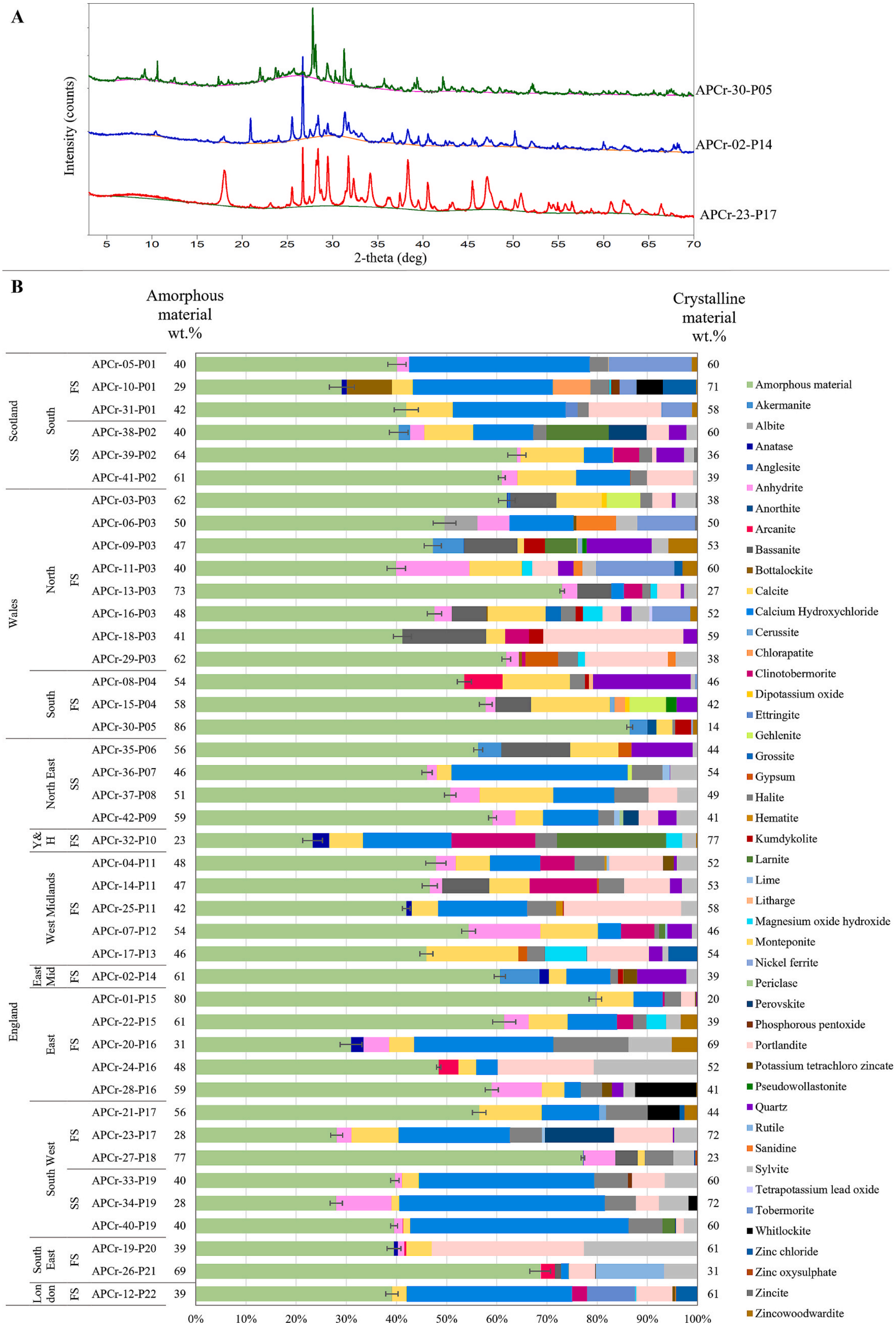

**Fig. 3. Mineralogy of UK APCr analysed by XRD.** A: Diffractograms of APCr samples with different contents of amorphous material evidenced by background deformations. B: Distribution of amorphous and crystalline fractions across 42 APCr samples. Crystalline contents were calculated as the sum of wt.% of all mineral phases. Amorphous fractions were estimated by deducting crystalline content from 100%. Error bars represent ± 1 standard deviation of the crystalline contents, calculated by propagating uncertainties of individual phases. England's regional labels are abbreviated as follows: 'Y&H' for Yorkshire and The Humber, and 'East Mid' for East Midlands; other region names are shown in full. FS denotes First Sampling; SS denotes Second Sampling.

### 3.4. Estimation of organic fraction by TOC and LOI

TOC and LOI are key indicators of organic matter in APCr. TOC reflects residual organic compounds originating from incomplete waste combustion and adsorbed volatile species, including dioxins and furans. LOI at 550°C indicates mass loss upon thermal treatment due to volatile organics, structural water and activated carbon introduced during flue gas cleaning processes. Fig. 4A presents TOC and LOI levels for 26 APCr samples, compared against hazardous WAC limits. TOC was detected in only seven samples (27% of the batch), with concentrations predominantly near the detection limit (1.6 mg/kg) and substantially below the WAC of 6 wt%, including samples from South Scotland, North Wales, West Midlands, and South West England. The single sample from East Midlands exhibited TOC approaching the WAC (6 mg/kg) and one of the samples from South Wales (APCr-15-P04) exceeded this threshold, indicating residual organics and potentially incomplete combustion. Since the few samples in which TOC was detected were distributed across the majority of the targeted regions, it can be stated that TOC might or might not be present at detectable concentrations in any event, however the probability to exceed the WAC remains as low as 3.8%.

LOI ranged from 0.0 wt% to 15.1 wt%, with 23 samples (84% of batch) below the 10 wt% threshold, suggest an overall trend of low levels of volatile or thermally decomposable components, consistent with effective incineration and gas treatment practices. Three atypical samples, APCr-18-P03 from North Wales, and APCr-08-P04 and APCr-15-P04 from South Wales, exceeded the LOI limit, likely due to the elevated contents of thermally decomposable phases such as portlandite ($Ca(OH)_2$) in APCr-18-P03 and bassanite ($CaSO_4 \cdot 0.5H_2O$) in APCr-15-P04 and APCr-18-P04, determined in the mineralogical analysis. The datasets show considerable variability, as illustrated in Fig. 4B, with CVs of 61% for TOC and 70% for LOI, and outliers corresponding to samples from Wales. The mean TOC value falls below the analytical detection limit, indicating that this parameter is generally expected to remain undetected. Whereas, the variability in LOI reduces the representativeness of its mean value. Nevertheless, the overall trend, marked by frequent compliance with hazardous WAC thresholds and rare TOC detection, suggests that UK APCr may offer promising potential for safe valorisation from an organic content perspective, based on the estimated total organic fraction. Future research should focus on a detailed characterisation of this fraction, including the identification and quantification of specific compounds or compound groups, such as dioxins and furans, and an assessment of their potential implications for management practices and recycling strategies.

### 3.5. Leaching tests

#### 3.5.1. Leaching of heavy metals

Leaching analyses of 26 APCr samples revealed concerns related to Ba, Cr, Cu, Mo, Pb and Zn. Fig. 5A compares their total and leachable concentrations against hazardous WAC limits. Although Zn and Pb are typically reported as the most problematic heavy metals in APCr (Fernández Bertos et al., 2004a), Pb emerged as the most critical in this study, exhibiting the highest leaching rates (7.0–2,569.5 mg/kg) and being the only metal that exceeded its hazardous WAC threshold. An exception was observed in South Wales, where none of the analysed samples released Pb. The elevated Pb leachability is attributed to the formation of soluble Pb-chlorides through chlorine complexation (Hjelmar, 1996), further promoted by APCr's alkaline pH in contact with water (Quina et al., 2008). Despite Zn exhibited higher total concentrations than Pb, its leachability was notably lower (max. 184.9 mg/kg),

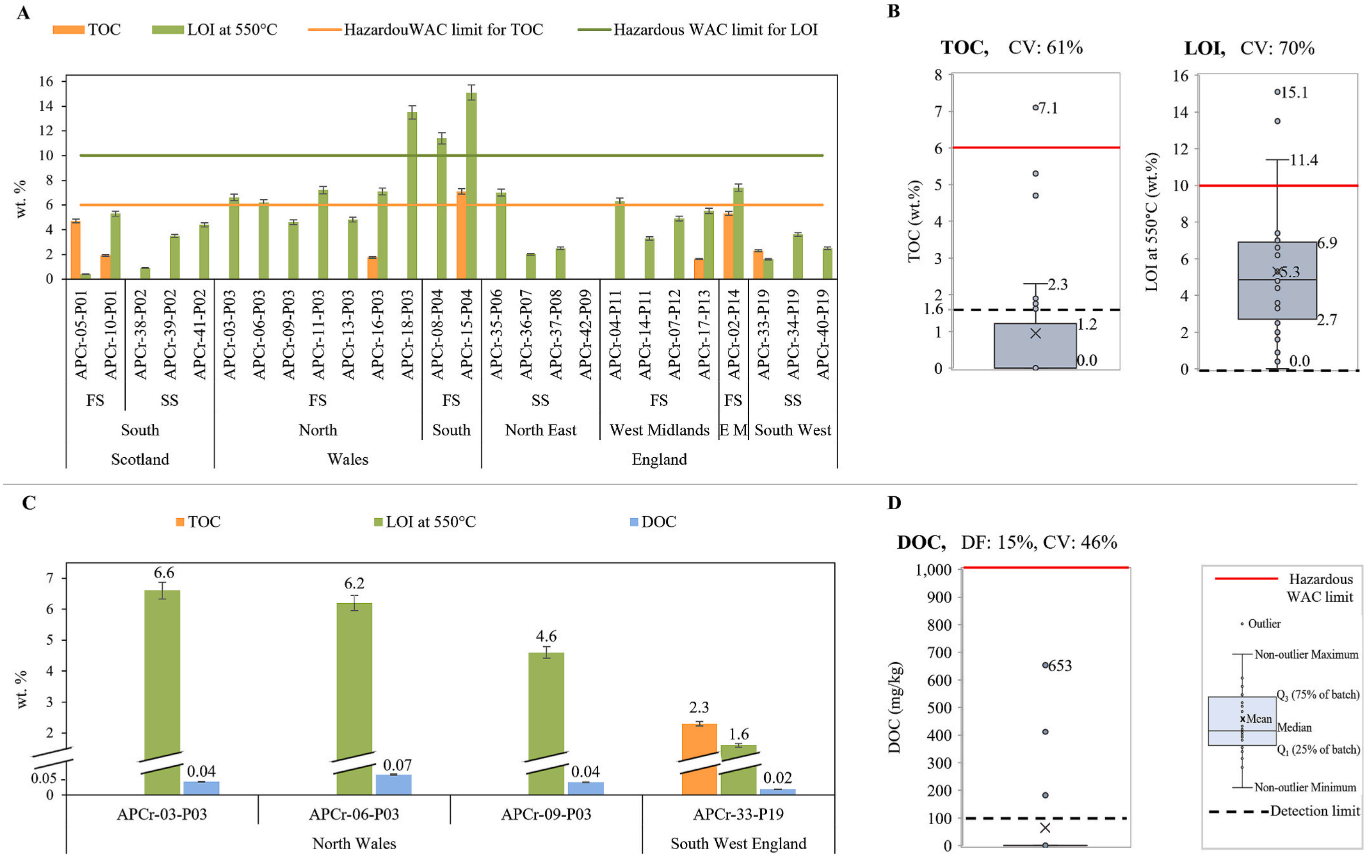

**Fig. 4. Estimation of organic fraction in UK APCr.** A: TOC and LOI across APCr samples, evaluated against WAC thresholds and variability analysis. B: DOC plotted against TOC and LOI, with variability analysis relative to WAC thresholds. Error bars represent ± 1 standard deviation, calculated by propagating uncertainties from sample processing and instrumental measurements.

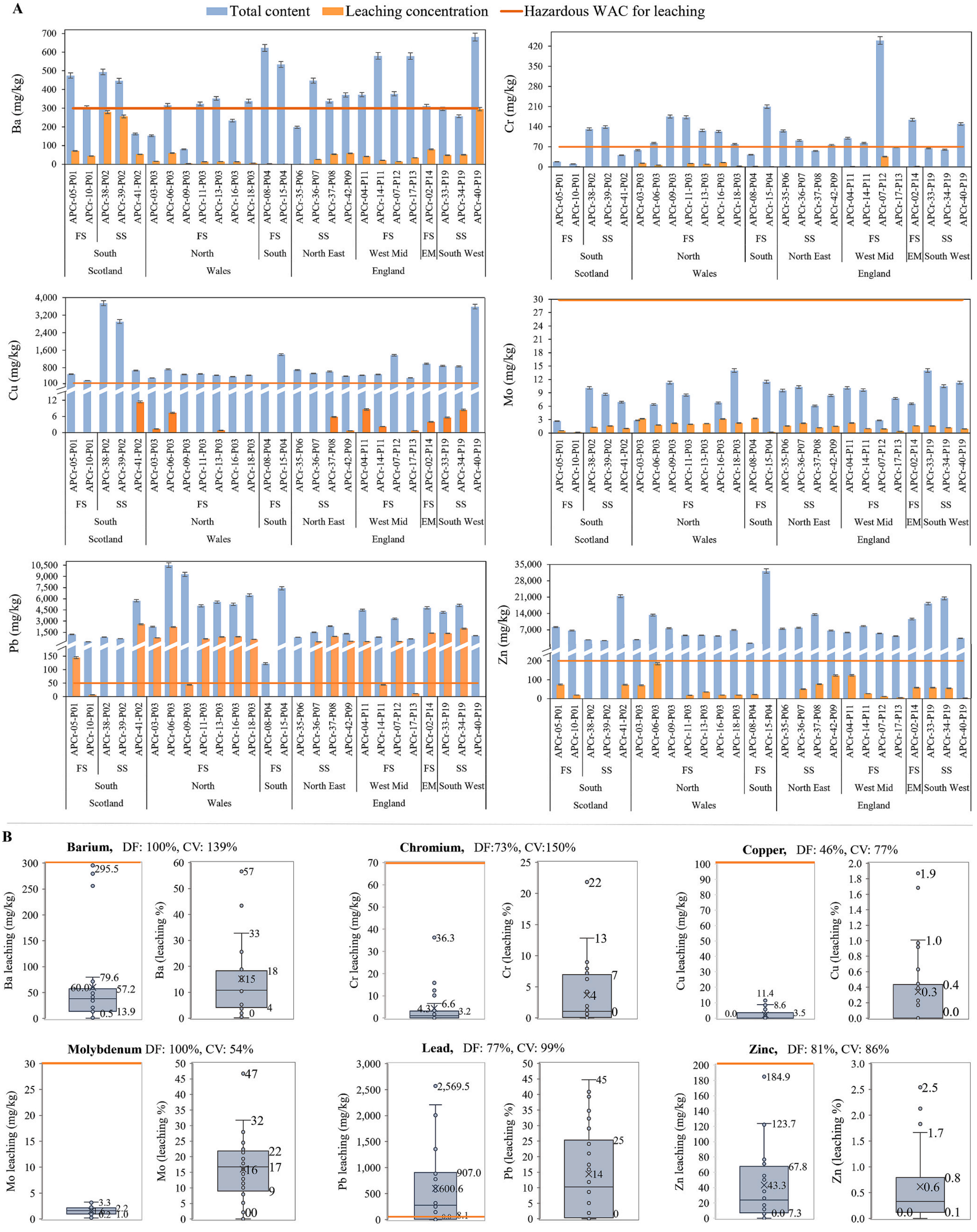

**Fig. 5. Leaching of environmentally concerning heavy metals from UK APCr (BS 12457–2:2002).** A: Leaching concentrations compared to total contents and WAC limits. Error bars represent ± 1 standard deviation, calculated by propagating uncertainties from sample processing and instrumental measurements. B: Variability analysis of leaching concentrations and leaching rates expressed as percentages. Leaching % = leaching x 100/total content.

consistent with reduced solubility under alkaline conditions (Ecke et al., 2002).

High total metal contents did not necessarily correlate with high leachability, complicating predictive assessments. For instance, although APCr-38-P02 and APCr-39-P02 from South Scotland, and APCr-40-P19 from South West England with elevated total Ba concentrations exhibited the highest Ba leaching, approaching its WAC limit of 300 mg/kg, other samples across the different regions with similar Ba contents released less than 100 mg/kg or did not release it. Similarly, APCr-06-P03 from North Wales, APCr-42-P09 from North East England and APCr-04-P11 from West Midlands, exhibited the highest Zn leaching rates despite having total Zn concentrations comparable to or lower than samples with minimal or non-detectable release of this metal. Notably, APCr-15-P04 from South Wales, which had the highest total Zn content showed no quantifiable Zn leaching. These discrepancies suggest that metal leachability in APCr is governed more by chemical speciation and mineralogical form than by total content, as previously observed by Quina et al. (2008). Elevated Ba and Zn leaching may indicate soluble compounds like $BaCl_2$, $ZnCl_2$ and $ZnSO_4$, while lower leachability may reflect stable forms such as $BaSO_4$ and ZnO. Zn and Ba, deserve close attention because atypical samples represent APCr streams posing environmental risks. Samples highly enriched in Cr and Cu (APCr-38-P02 and APCr-39-P02 from South Scotland and APCr-40-P19 from South West England), did not release these metals, likely due to presence of stable $Cr^{3+}$ species and CuO. In contrast, Cr and Cu leaching from other samples may be linked to more soluble $Cr^{6+}$ compounds and Cu-chlorides. Mo leaching remained consistently below 3 mg/kg across all targeted UK regions, probably reflecting minor concentrations of molybdite ions $(MoO_4)^{2-}$ under the alkaline conditions of APCr, despite no Mo-based crystalline phases being detected in the solid material.

Among the other metals regulated for landfill disposal, Se was detected only in leachate APCr-10-P01 from South Scotland (2.3 mg/kg), while Cd was identified in leachates APCr-37-P08 from North East England and APCr-41-P02 from South Scotland (0.1 mg/kg each). All values were below the hazardous WAC limits (7 mg/kg for Se, 5 mg/kg for Cd). As (<1.582 mg/kg), Hg (<1.158 mg/kg), Ni (<0.325 mg/kg) and Sb (<0.858 mg/kg) were not detected in any leachate, consistent with previous finding by Gunning et al. (2011). These results indicate that Se, Cd, As, Hg, Ni, and Sb pose minimal environmental concern in UK APCr.

Leaching variability for the six environmentally concerning metals was assessed (Fig. 5B). Ba, Cr, Mo, Pb and Zn were consistently detected in 73 – 100% of APCr leachates, while Cu appeared in less than half. Pb was confirmed as the most critical heavy metal with nearly 75% of leaches exceeding the hazardous WAC threshold. Ba exhibited relatively low leachable concentrations, with almost 75% of leachates values below 60 mg/kg, less than one-fifth of its WAC limit, despite a few outliers corresponding to samples from South Scotland and South West England. Zn presented only one outlier (a sample from North Wales), while 75% of leaching values remained at below 124 mg/kg, well under the WAC threshold. Cr displayed the broadest dispersion in leaching concentrations, reaching 36 mg/kg (including a few outliers from West Midlands and North Wales), around 50% of its WAC limit. Mo and Cu, although variable, showed the lowest leachable concentrations, each representing about 10% of their respective WAC thresholds. Overall, these findings indicate that the environmentally concerning metals are consistently released from APCr, although Pb is the only element exceeding WAC limits. To provide a broader interpretation, leaching was expressed as a percentage of total metal content, yielding mean values for UK APCr: Mo (16%), Ba (15%), Pb (14%), Cr (4%), Zn (0.6%) and Cu (0.3%). These mean leaching ratios may serve as indicators of UK APCr environmental behaviour and inform future studies on management and valorisation strategies.

### 3.5.2. Leaching of soluble salts and TDS

Fig. 6A presents the leaching rates of chlorides, sulphates, fluorides and TDS in 26 APCr samples, compared against hazardous WAC limits. Chloride leaching was observed in 25 samples (96% of the batch) across all targeted UK regions and emerged as the primary environmental concern since 88% of samples exceeded the 25,000 mg/kg hazardous WAC limit. Chloride leachable concentrations primarily oscillated around 100,000 mg/kg, but some samples from South Scotland, and the North East and South West of England exceeded 200,00 mg/kg. Chloride leaching rates reflected the presence of major chloride-bearing species including NaCl, KCl, and mainly CaOHCl, as determined in the mineralogical analysis. APCr-15-P04 from South Wales was the sole leachate in which chlorides were not detected, consistent with the absence of chloride salts in its solid matrix. Chloride leaching rates accounted for approximately half of TDS, highlighting their disproportionate impact. These finding underscore chloride mitigation as a critical priority in APCr management, whether for disposal or valorisation.

Sulphate leaching was detected in all APCr samples, ranging from 53.0 to 27,566.2 mg/kg, well below the 50,000 mg/kg hazardous WAC limit. Leachable concentrations were predominantly around 18,000 mg/kg, with notable exceptions in APCr-38-P02 and APCr-39-P02 from South Scotland and APCr-40-P19 from South West England, which exhibited markedly lower values (177, 173 and 53 mg/kg, respectively), reflecting reduced sulphate-bearing mineral phases. Sulphates contributed significantly less to TDS than chlorides, representing about one-eighteenth of the total. Key leaching phases, based on the mineralogical analysis, included calcium sulphate variants ($CaSO_4$, $CaSO_4{\cdot}0.5H_2O$ and $CaSO_4{\cdot}2H_2O$) and arcanite ($K_2SO_4$), given their moderate solubility. Although within regulatory limits, sulphate leaching remains substantial and requires attention during APCr management.

Fluoride leaching was detected in 62% of APCr samples across all targeted regions except South Wales, with concentrations ranging from 22.8 to 43.9 mg/kg, mostly below 35 mg/kg and well below the 500 mg/kg hazardous WAC limit. At these levels, fluoride contribution to TDS is negligible and environmental risk is probably minimal. Since no fluoride-bearing minerals were detected in the APCr matrix, the leaching species remain uncertain. Likely NaF, KF or $CaF_2$ formed during flue gas neutralisation, remaining undetectable in the solid residues but sufficiently soluble to appear in the leachates.

Leaching data for soluble species in APCr showed substantial variability, consistent with mineralogical findings and illustrated in Fig. 6B boxplots. CVs exceeded 50% for chlorides, sulphates and TDS, and reached 20% for fluorides, indicating inconsistent patterns and reducing the reliability of average leachable concentrations. Instead, the observed ranges offer useful screening of total leachable loads of soluble salts and TDS, essential for assessing environmental risks in recycling or landfilling. The scatterplot in Fig. 6B shows a strong positive correlation between TDS and conductivity in APCr leachates, since most data points cluster along a linear trend. This confirms conductivity as a reliable proxy for estimating ionic strength and leaching potential, dominated by soluble chlorides and sulphates. Hence, conductivity screening offers a practical method for classifying APCr batches and identifying those requiring targeted treatment, such as washing, stabilization, or encapsulation, to reduce leaching and ensure compliance. Also, the conductivity range (1,875–60,960 μS/cm) expands on Robinson et al. (2004), who reported values from 46,000 to 56,000 μS/cm.

### 3.5.3. DOC

Despite TOC and LOI levels occasionally exceeded hazardous WAC limits, the leachable organic fraction, quantified as DOC, was detected in only four the 26 APCr eluates (15% of the batch), with concentrations consistently below the 1,000 mg/kg regulatory threshold (Fig. 4D). For these samples, which originated from North Wales and Sout West England, DOC was expressed as wt.% and compared with TOC and LOI (Fig. 4C), revealing negligible proportions. Notably, the –PO3 samples from North Wales that released DOC lacked measurable TOC in the solid matrix, suggesting that DOC likely originated from residual activated carbon or unburnt organic matter, rather than dioxins or furans. This

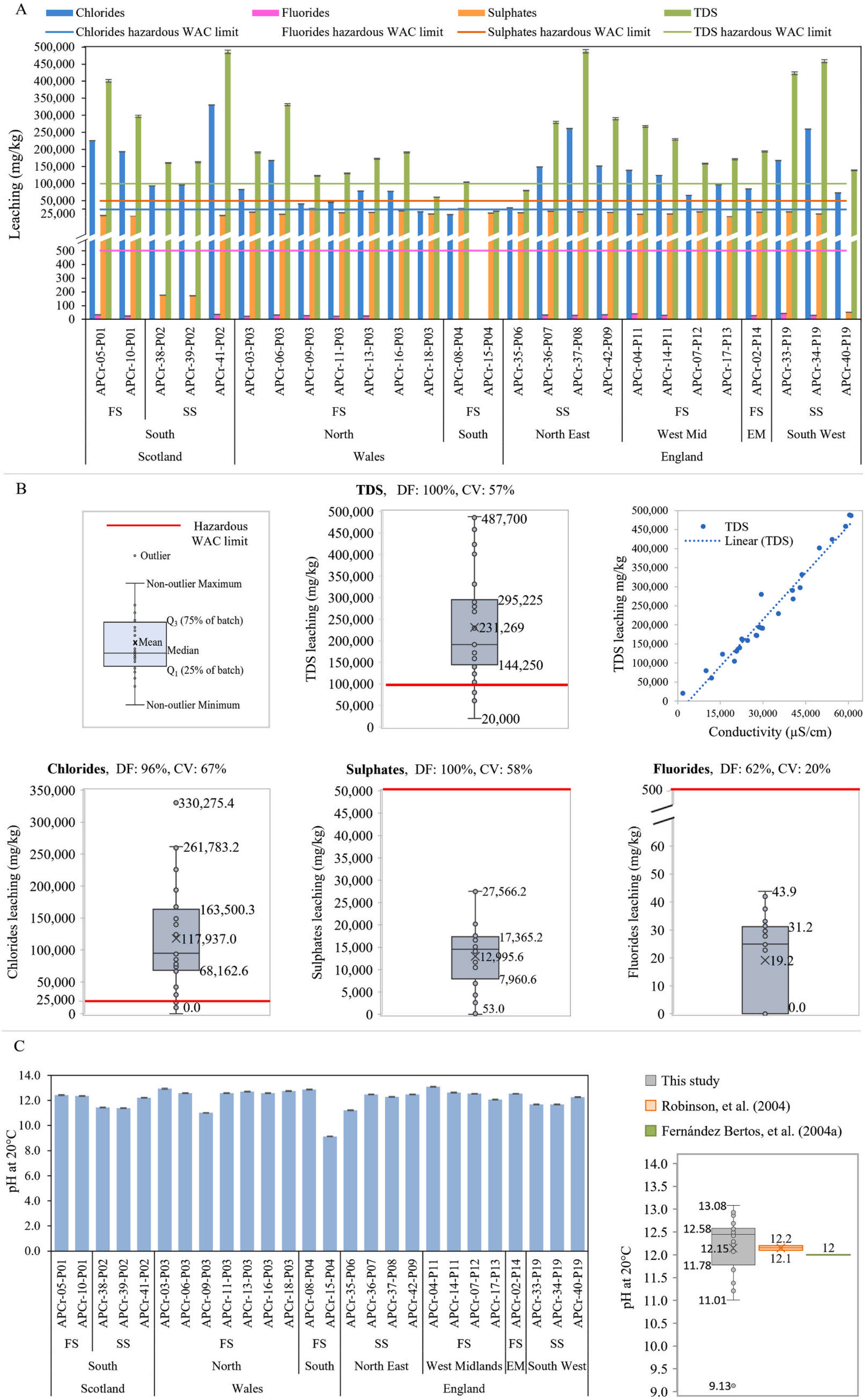

**Fig. 6.** Leaching behaviour of UK APCr (BS 12457–2:2002). A: Soluble salts and TDS compared against hazardous WAC thresholds. B: Variability in leaching rates of soluble salts and TDS, and correlation between leachate conductivity and TDS. C: pH values across samples and variability contextualized with UK studies. The pH value attributed to Fernández Bertos et al. (2004a) was estimated from graphical data. Error bars in A and C represent ± 1 standard deviation, calculated by propagating uncertainties from sample processing and instrumental measurements.

aligns with Robinson et al. (2004) who reported DOC concentrations of 4–5 mg/L, with no detection of dioxins and furans in UK APCr leachates. The absence of DOC in most eluates and the minimal leachable concentrations detected, indicate that the APCr organic fraction remains predominantly immobilised in the solid matrix. Therefore, UK APCr is unlikely to pose significant environmental risks from organic pollutant leaching. These findings reinforce its safe valorisation, particularly through cold bonding processes such as accelerated carbonation, where organic removal is not targeted. Nevertheless, a comprehensive screening of organic compounds in APCr leachates is recommended to confirm their occurrence, assess their potential leaching behaviour, and further substantiate the safe valorisation of APCr.

### 3.5.4. pH

Fig. 6C bar chart shows that APCr leachates are highly alkaline, with pH values mostly between 12 and 13, aligning with previous UK studies which reported pH values around 12. The elevated alkalinity results from $Ca(OH)_2$, CaO and $NaHCO_3$ additions during flue gas neutralisation, along CaOHCl formation. Samples APCr-38-P02 and APCr-39-P02 from South Scotland showed slightly lower pH (around 11.5) resulting from reduced contents of $Ca(OH)_2$ and CaOHCl. Samples APCr-09-P03 and APCr-15-P03 from North Wales and APCr-35-P06 from North East of England exhibited further reductions due to absence of alkaline phases and enrichment in $CaSO_4 \cdot 0.5H_2O$, $CaCO_3$, $SiO_2$ and Ca-silicates. Despite these variations, pH dispersion was low (CV = 7%), indicating consistent high alkalinity. Fig. 6C boxplot confirms that overall, UK APCr leachates exhibit pH values between 11 and 13, averaging 12.15 at 20°C. High pH in APCr leachates significantly influences contaminant mobility. Under strong alkaline conditions ($pH \geq 8$), non-amphoteric metal ions such as Cd, Cu and Ni, precipitate as hydroxides or carbonates, reducing their solubility, while amphoteric metals such as Pb and Zn redissolve (Quina et al., 2009; Sabbas et al., 2003). Oxy-anion forming elements, including As, Cr, Mo and Sb, generally decrease in solubility at pH values above 10 (Sabbas et al., 2003). Chloride solubility is not pH–dependent (Quina et al., 2009). Consequently, chloride leaching from the analysed APCr remained consistently high. In contrast, sulphate mobility shows some pH sensitivity. At high pH, sulphates are incorporated into stable ettringite ($Ca_6Al_2(SO_4)_3(OH)_{12} \cdot 26H_2O$), but as pH decreases, particularly below 10, ettringite decomposes, leading to increased sulphate release (Quina et al., 2009). This can explain the low sulphate leaching observed for APCr-12-P22 from London, which was exceptionally enriched in ettringite.

### 3.5.5. Environmental impact of UK APCr

APCr generated during MSW incineration represent a critical stage in the EfW life cycle due to their hazardous composition and environmental implications. For a Life Cycle Assessment (LCA), APCr management, whether disposal or recycling, becomes the main environmental hotspot, as treatment choices strongly influence overall impacts. The UK APCr characterisation conducted in this study revealed complex chemical and mineralogical profiles with leaching behaviour. Despite high variability in samples across different EfW facilities and UK geographical areas complicating environmental risk predictions, marked tendencies allowed identification of significant risks. Chlorides, primarily CaOHCl, NaCl, and KCl, dominate environmental concerns, since 88% of samples exceeded hazardous WAC for chloride leaching. Chloride release is associated with reduced soil fertility, aquatic toxicity, and groundwater corrosivity (Xia, 2021). In recycling into construction applications, such as lightweight aggregates incorporating APCr, chloride migration into concrete can accelerate steel reinforcement corrosion, causing expansion and cracking of the structural matrix (Engineering Notes, 2023). Sulphates, though below WAC thresholds, remain problematic, potentially contributing to toxicity in water bodies surrounding landfills. In construction applications, sulphate attack due to leaching can compromise concrete integrity through expansion, cracking, and softening (Bai, 2016; Building Research Establishment, 2008). Fluoride release, while compliant, persists at low levels, warranting precautionary treatment to mitigate environmental release. Fluoride leaching can degrade groundwater quality, making it unsuitable for drinking purposes. It can also pose toxicity risks through plant bioaccumulation (Singh et al., 2018). The highly alkaline nature of APCr leachates (pH 11–13) amplifies these risks by increasing the solubility of certain species, primarily lead. Pb emerged as the most critical heavy metal, exceeding WAC limits in over 75% of leachates due to formation of soluble Pb-chlorides under alkaline conditions. Other metals such as Zn, Ba, and Cr occurred at notable concentrations but exhibited lower leachability, indicating that in APCr, chemical speciation of the solid matrix governs environmental behaviour more than total content. Organic pollution appears less concerning since TOC and DOC levels were generally below hazardous thresholds, suggesting minimal risk. Nevertheless, POPs, like dioxins and furans, can cause long-term contamination in groundwater and surface water systems, even at trace levels, requiring costly remediation.

From an LCA perspective, these findings underscore the need for improved treatment strategies to mitigate chloride, sulphate and lead leaching. Established methods such as stabilisation – solidification remain essential, while emerging approaches like washing and accelerated carbonation can offer pathways for reducing environmental impacts and enabling APCr valorisation. Integrating these strategies into APCr management supports regulatory compliance and aligns with circular economy goals, transforming APCr from a disposal challenge into a resource within sustainable material cycles.

## 3.6. Microstructure and local elemental composition

### 3.6.1. Fine-grained material

APCr mainly consisted of fine-grained material (Fig. 7A) with particle sizes ranging from 0.1 to 1 μm, mostly composed of O, Ca and Cl, with presence of S, K, Mg, Na, Si, Zn, Al, Fe, Cu and P. Unshaped particles were the dominant structures, though spheres, cubes and other geometric forms were present. CaOHCl phases appeared as block-like structures (about 10 μm) and spheres (<1μm diameter), as previously described by Bogush et al. (2015). Layered blocks of CaOHCl with around 1 μm thick layers are shown in Fig. 7B. Fine particles adhered to larger surfaces, often obscuring morphology and complicating structural identification

### 3.6.2. Spherical particles

Plain spherical particles (Fig. 7C), 10–130 μm, were primarily composed of O, Si and Ca, with moderate concentrations (1–5 wt%) of Fe, Al, Na, K, Cl, Zn, S, Mg, and small quantities (<1 wt%) of Pb, Ti, Cu, P and Mn. Identified as aluminosilicates by Bogush et al. (2015), SEM-EDS mapping confirmed they are Ca-aluminosilicates. Holey speres (Fig. 7D), 55–62 μm, showed similar composition but were enriched in K over Ca and contained fine Ca-rich within their cavities. These are K-aluminosilicates, specifically sanidine ($KAlSi_3O_8$), detected in 12% of samples. Hemispherical particles with non-concentric hollow regions (14–86 μm), were observed in several APCr samples. Two distinct types were identified: one exhibited a thick shell rich in O, Ca, and S, with a shallow central cavity (Fig. 7E); the other displayed a thinner shell enriched in O, Si, Ca, and Fe, and a deeper hollow containing fine Ca-rich impurities (Fig. 7F). Their elemental composition resembled plain and holey spheres, including both prevalent and secondary elements. Morphologically, these particles are likely fragmented spheres, revealing internal microstructure and elemental distribution. Hollow spherical particles, known as cenospheres (11–14 μm), were found in APCr samples, typically appearing as perfectly rounded spheres with a hole (Fig. 7G). Composed mainly of O, Ca and Si, they also contained moderate concentrations of Fe, Al and Mg, and lower amounts of P, S, Mn, Cl and Na. Cenospheres appeared consistently covered with fine Ca-rich material, possibly affecting surface integration with other particles.

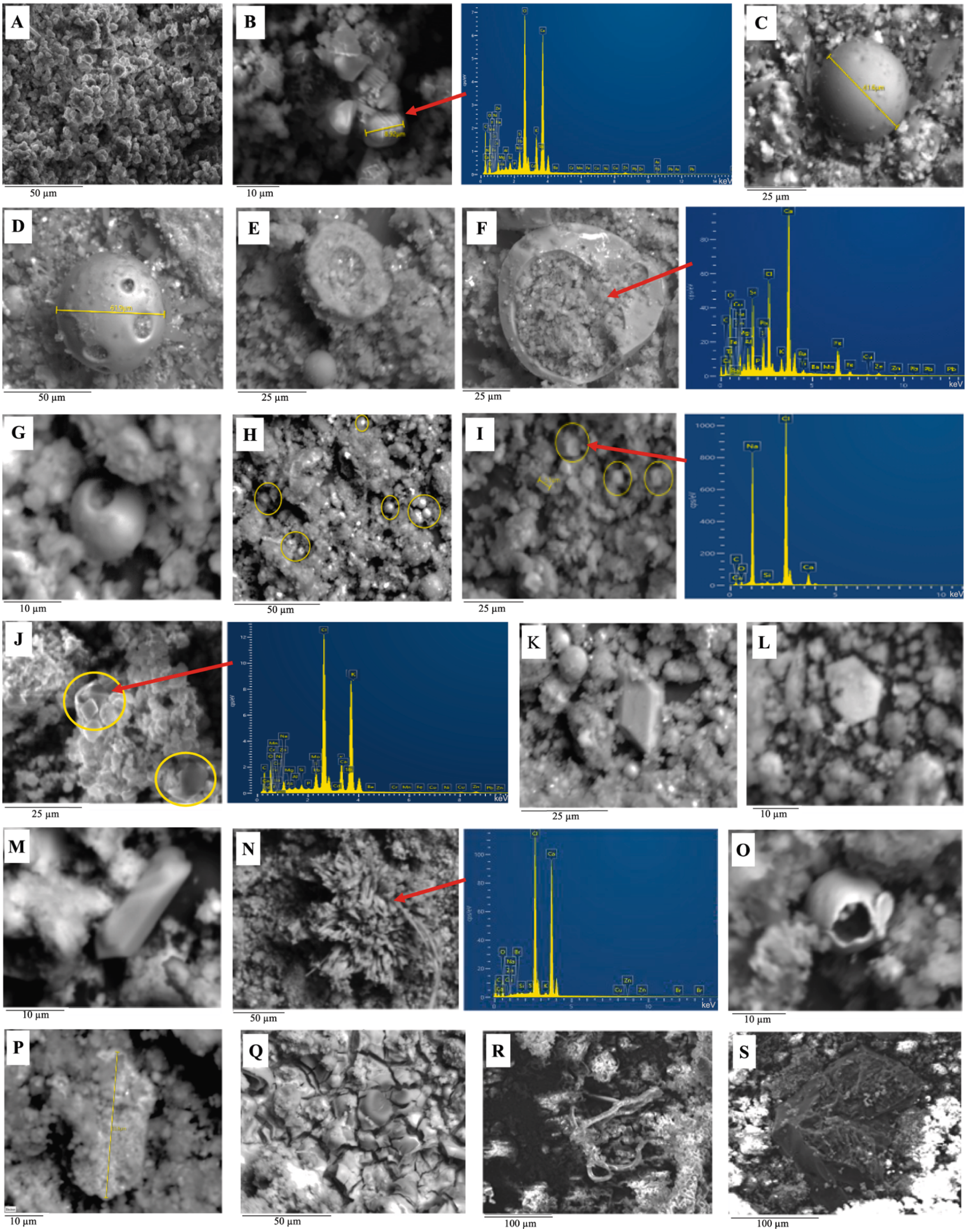

**Fig. 7. SEM micrographs and SEM-EDS spectra of different particles of APCr.** A: Fine-grained matrix with heterogeneous particles: irregular, spherical, cubic, and angular morphologies, B: Layered blocks of fine-grained material corresponding to CaOHCl, C: Plain-surfaced spheres composed of Ca-aluminosilicate phase, D: Hollow K-aluminosilicate spheres with Ca-rich internal inclusions, E: Thick-shelled hemisphere enriched in O, Ca and S, with a shallow cavity, F: Thin-shelled hemisphere enriched in O, Si, Ca, Fe, with a deep Ca-rich cavity, G: Hollow sphere (cenosphere) exhibiting surface aperture and composed of aluminosilicate phase, H: Fine spheres within fine-grained material corresponding to CaOHCl morphological variants, I: Cubic particles of NaCl within fine-grained material, J: Octahedral bipyramids of KCl within fine-grained material, K: Rhombohedral particle corresponding to $CaSO_4 \cdot 2H_2O$, L: Hexagonal particle corresponding to a crystal shape of $CaCO_3$, M: Bladed single particle, likely a morphological variant of CaOHCl, N: Needle-like aggregate of bladed particles, O: Spherical shell (ferrosphere) composed of ferro-oxides, P: Laminar fragment composed of $TiO_2$ likely in rutile phase, Q: Crushed aluminium foil laminas with fine-grained material within fissures, R: Fibres of aluminium foil tangled among fine-grained material, S: Fragment of unburnt organic matter with fine-grained material on its surface.

Their composition aligns with aluminosilicate phases present in incineration residues. Due to their hollow structure (filled with air or inert gases), cenospheres offer low density, high thermal stability and strength (Ranjbar and Kuenzel, 2017), ideal for potential use in lightweight construction materials. The smallest spherical particles (1–10 μm), observed within the fine-grained APCr fraction (Fig. 7H), were mainly composed of O, Ca and Cl, with minor amounts of K and Na. Their elemental profile and widespread occurrence suggest they are morphological variants of CaOHCl, consistent with Bogush et al. (2015).

### 3.6.3. Crystalline forms and aggregates

Cubic particles (about 5 μm) were found within the fine-grained APCr matrix (Fig. 7I), composed of Na and Cl, consistent with NaCl. Octahedral bipyramids (about 6 μm), composed of K and Cl, were observed in a few APCr samples (Fig. 7J) and identified as KCl. Although mineralogical analysis confirmed NaCl and KCl in 76% and 79% of samples respectively, SEM imaging was challenging due to their brightness and small size, which reduced contrast against surrounding fine material. Rhombohedral particles (about 30 μm), shown in Fig. 7K, were mainly composed of O, Ca and S, corresponding to $CaSO_4{\cdot}2H_2O$, a contributor to sulphate leaching. Hexagonal particles (about 13 μm) found in some APCr samples (Fig. 7L), were primarily composed of Ca, O and C, consistent with $CaCO_3$. Although $CaCO_3$ can exhibit various crystal shapes, only the hexagonal form was observed under the analytical conditions used. Bladed particles mainly composed of Ca, Cl, and O, were present in most APCr samples. These were rarely isolated (Fig. 7M), more commonly as part of larger needle-like aggregates (Fig. 7N),and are likely a form of CaOHCl.

### 3.6.4. Metallic particles

Spherical shells (around 15 μm) and fragmented shell pieces, mostly composed of Fe, were observed across several APCr samples (Fig. 7O). Known as ferrospheres, these particles are typical of incineration residues They form when Fe-based components from electronic and electrical waste (e.g. wires, filaments, meshes) evaporate during combustion and then recondense. Ferrospheres are classified by Fe content: ferro-oxides (>75% Fe), aluminosilicate-bearing ferro-oxides (50–75% Fe), high ferriferous aluminosilicates (25–50% Fe) and ferro-aluminosilicates (<25% Fe) (Zhao et al., 2006). In the analysed APCr, ferrospheres contained around 80% Fe, indicating a predominance of ferro-oxides, likely non-crystalline iron (III) oxide ($Fe_2O_3$) often formed during combustion processes.

A laminar particle (around 34 μm) identified in one sample (Fig. 7P) was composed of 82% Ti with lower amount of O and surrounded by impurities including Ca, Zn, K, Al, Fe, Cl, S and Na. Likely rutile ($TiO_2$), it formed through thermal transformation of Ti-based compounds from plastics, coated papers and packaging. Although $TiO_2$ was detected in only 10% of samples via XRD, this marks the first reported occurrence in UK APCr, reflecting mineralogical diversity and incorporation of elements from heterogeneous waste streams.

Aluminium fragments, including crushed laminas (Fig. 7Q) and fibres (Fig. 7R), were found in various APCr samples. Fine-grained material rich in O, Ca and Cl, was deposited on Al surfaces, especially within cracks, while Al fibres appeared tangled among fine material aggregates. These originated from incinerated Al-bearing products such as foil, packaging and coatings. During combustion, Al can oxidise or fragment, melt and re-solidify into distorted shapes captured by the APC system. Though not regulated under WAC, Al was detected in 90% of the samples, reaching 9.2 wt%. Its widespread presence contributes to APCr's chemical complexity and indicates potential for targeted metal recovery.

### 3.6.5. Unburnt organic matter

Laminar fragments of unburnt organic matter with wrinkled, porous surfaces (Fig. 7S) were found in most APCr samples. Fine-grained material rich in Ca, Na, P, Si, Zn, Al, Mg and Fe appeared deposited within these surface features. Originating from incomplete combustion of organic-rich MSW (e.g. vegetation, food, packaging and plastics), these fragments contributed to LOI and may have served as a source of DOC in leachates where detected.

## 4. Conclusions

This study provides the first systematically characterisation of UK APCr across a broad sample set, analysing 42 APCr samples from 22 UK EfW facilities in Scotland, Wales and England. APCr consistently contained high levels of O, Ca, Cl and Si, with frequent detection of Al, Mg, Fe, P, S, Zn, K and Na. Ten WAC-regulated metals, As, Ba, Cd, Cr, Cu, Mo, Ni, Pb, Sb and Zn, were commonly present, while Hg and Se were rarely detected. Mineralogical analysis identified 45 phases, including 21 newly reported in APCr. Dominant crystalline phases included $CaSO_4$, $CaCO_3$, CaOHCl, $Ca(OH)_2$, NaCl, KCl and $SiO_2$, alongside Si-rich minerals such as clinotobermorite ($Ca_5H_8O_{21}Si_6$), larnite ($Ca_2SiO_4$) and sanidine ($KAlSi_3O_8$). APCr from South Scotland, North Wales, Yorkshire and The Humber, the West Midlands, South West and South East England, and London contained over 50% crystalline material, while residues from South Wales, North East England, the East Midlands, and the East of England were mainly amorphous. Despite substantial variability across EfW facilities and regions, several consistent environmental risks were identified. Leaching tests revealed elevated releases of Ba, Cr, Cu, Mo, Pb, Zn, chlorides and sulphates. Among these, Pb and chlorides most frequently exceeded hazardous WAC leaching limits, posing the greatest environmental risk from APCr. The strongly alkaline nature of APCr leachates (pH 11–13) explained the solubility of certain species, particularly lead. In contrast, organic fraction estimation showed TOC predominantly undetected, LOI largely below hazardous WAC limits and DOC absent in most of eluates, suggesting that organic pollutants, mostly remain immobilised in the solid matrix. Microstructural observations confirmed a fine-grained, partially amorphous material with heterogeneous particle morphologies (spheres and crystalline forms) and inclusions of unburnt organics, carbon residues and metals, reflecting the complex formation pathways of APCr. These findings establish a robust baseline on UK APCr composition, behaviour and valorisation potential, providing essential evidence to support safer and more sustainable management strategies.

Building on these conclusions, several priority areas emerge for advancing APCr management, treatment and valorisation in the UK. The combined elemental, mineralogical and leaching evidence highlights the need to mitigate the mobility of key contaminants, particularly highly soluble salts (CaOHCl, NaCl, KCl and $CaSO_4$ variants) and environmentally concerning metals such as Pb, Zn, Ba, Cr, Mo and Cu. Given their consistently elevated leaching, Pb, Zn and Ba require focused investigation to investigate the mechanisms governing their release and to support the development of targeted treatment pathways. The stable fraction, including the amorphous phase and newly identified Si–bearing minerals, also requires deeper investigation to support their potential benefits to the engineering performance of APCr–derived materials, such as supplementary cementitious materials or alkali–activated binders. The high Si–bearing content in APCr from Yorkshire and The Humber, along with the strong compositional variability in Wales, also enriched with Si-based mineral, make these streams particularly valuable for future investigation. In parallel, the enrichment of Fe, Ti and Al in the APCr microstructure, deserves evaluation as opportunity for resource recovery as part of resource–efficiency strategies. Although this study provides foundational mineralogical and leaching data for integrated analyses linking amorphous phase composition with long–term stability, the amorphous fraction remains insufficiently characterised. Future work should incorporate complementary analytical techniques to elucidate structural disorder, bonding environments, hydration states and thermal behaviour of non–crystalline and poorly crystalline components. Such insights are critical for predicting APCr long term stability, reactivity and performance in both environmental and valorisation contexts. The substantial intra–batch variability and few consistent regional trends reflected the dynamic nature of APCr generation across EfW facilities. Therefore, batch–level assessments, as applied in this study, are recommended for future work. The generalisable indicators identified in this work, including mean heavy–metal leaching rates, can inform future environmental assessments nationwide management strategies. From an organic–content perspective, although the leaching risk appeared low, a comprehensive screening of organic compounds, particularly dioxins and furans, in both solid residues and eluates is recommended to confirm their occurrence and ensure safe valorisation. Finally, emerging treatment approaches such as washing and accelerated carbonation merit further investigation as promising routes for reducing environmental impacts while enabling APCr recycling. Their optimisation should be informed by the mineralogical and leaching insights generated in this study.

## CRediT authorship contribution statement

**Ximena Chamorro Bolaños:** Writing – review & editing, Writing – original draft, Visualization, Validation, Methodology, Investigation, Formal analysis, Data curation, Conceptualization. **Bamdad Ayati:** Writing – review & editing, Supervision, Resources, Project administration, Methodology, Conceptualization. **Darryl Newport:** Writing – review & editing, Supervision, Resources, Project administration, Funding acquisition, Conceptualization.

## Declaration of competing interest

The authors declare that they have no known competing financial interests or personal relationships that could have appeared to influence the work reported in this paper.

## Acknowledgements

This work was supported by a partnership between the Sustainability Research Institute at the University of East London and Augean, United Kingdom. The authors gratefully acknowledge Gene Wilson, Gary Bower and Chris Franklin of Augean for their continuous collaboration and valuable feedback throughout the study.

## Appendix A. Supplementary data

Supplementary data to this article can be found online at https://doi.org/10.1016/j.wasman.2026.115406.

## Data availability

Data will be made available on request.

## References

Abbas, Z., Moghaddam, A.P., Steenar, B.-M., 2003. Release of salts from municipal solid waste combustion residues. Waste Manag. 23 (4), 291–305. https://doi.org/10.1016/S0956-053X(02)00154-X.

Alba, N., Gassó, S., Lacorte, T., Baldasano, J., 1997. Characterization of municipal solid waste incineration residues from facilities with different air pollution control systems. J. Air Waste Manage. Assoc. 47 (11), 1170–1179. https://doi.org/10.1080/10473289.1997.10464059.

Araizi, P.K., Hills, C.D., Maries, A., Gunnin, P.J., Wray, D.S., 2016. Enhancement of accelerated carbonation of alkaline waste residues by ultrasound. Waste Manag. 50, 121–129. https://doi.org/10.1016/j.wasman.2016.01.006.

Ashraf, M.S., Ghouleh, Z., Shao, Y., 2019. Production of eco-cement exclusively from municipal solid waste incineration residues. Resour. Conserv. Recycl. 149, 332–342. https://doi.org/10.1016/j.resconrec.2019.06.018.

Atanes, E., Cuesta-García, B., Nieto-Márquez, A., Fernández-Martínez, F., 2019. A mixed separation-immobilization method for soluble salts removal and stabilization of heavy metals in municipal solid waste incineration fly ash. J. Environ. Manage. 240 (15), 359–367. https://doi.org/10.1016/j.jenvman.2019.03.122.

Augean, 2024. Treatment & Disposal Services: APCr Treatment – Environmental Innovation. https://www.augean.co.uk/services/apcr/ (accessed 26 October 2024).

Baciocchi, R., Costa, G., Di Bartolomeo, E., Polettini, A., Pomi, R., 2009. The effects of accelerated carbonation on $CO_2$ uptake and metal release from incineration APC residues. Waste Manag. 29 (12), 2994–3003. https://doi.org/10.1016/j.wasman.2009.07.012.

Bai, J., 2016. Durability of Sustainable Construction Materials, in: Khatib, J. M. (Ed.), Sustainability of Construction Materials (Second Edition). Woodhead Publishing Series in Civil and Structural Engineering, pp. 397-414. https://doi.org/10.1016/B978-0-08-100370-1.00016-0.

Bodénan, F., Deniard, P., 2003. Characterization of flue gas cleaning residues from European solid waste incinerators: assessment of various Ca-based sorbent processes. Chemosphere 51 (5), 335–347. https://doi.org/10.1016/S0045-6535(02)00838-X.

Bogush, A., Stegemann, J., Roy, A., 2019. Changes in composition and lead speciation due to water washing of air pollution control residue from municipal waste incineration. J. Hazard. Mater. 361, 187. https://doi.org/10.1016/j.jhazmat.2018.08.051.

Bogush, A., Stegemann, J., Wood, I., Roy, A., 2015. Element composition and mineralogical characterisation of air pollution control residue from UK energy-from-waste facilities. Waste Manag. 36, 119–129. https://doi.org/10.1016/j.wasman.2014.11.017.

BS 3406-1:1986. Methods for determination of particle size distribution - Part 1: Guide to powder sampling. The British Standards Institution, London.

BS EN 12457-2:2002. Characterisation of waste. Leaching. Compliance test for leaching of granular waste materials and sludges. One stage batch test at a liquid to solid ratio of 10 l/kg for materials with particle size below 4 mm (without or with size reduction). The British Standards Institution, London.

BS EN 13137:2001. Characterisation of waste. Determination of Total Organic Carbon (TOC) In waste, sludges and sediments. The British Standards Institution, London.

BS EN 13657:2002. Characterisation of waste - Digestion for subsequent determination of aqua regia soluble portion of elements. The British Standards Institution, London.

BS EN 15934:2012. Sludge, treated biowaste, soil and waste. Calculation of dry matter fraction after determination of dry residue or water content. The British Standards Institution, London.

BS EN 15935:2021. Soil, waste, treated biowaste and sludge. Determination of loss on ignition. The British Standards Institution, London.

Building Research Establishment, 2008. Sulfate damage to concrete floors on sulfate-bearing hardcore: Identification and Remediation. RIBA Publishing, London. https://assets.publishing.service.gov.uk/media/5a7f1bf2e5274a2e8ab4a2b6/sulphate_damage_research_report.pdf.

Cao, Y.N., Luo, J.J., Sun, S.Q., 2021. Characteristics of MSWI fly ash with acid leaching treatment. J. Fuel Chem. Technol. 49 (8), 1208–1218. https://doi.org/10.1016/S1872-5813(21)60119-6.

Chen, W.-S., Chang, F.-C., Shen, Y.-H., Tsai, M.-S., Ko, C.-H., 2012. Removal of chloride from MSWI fly ash. J. Hazard. Mater. 237–238, 116–120. https://doi.org/10.1016/j.jhazmat.2012.08.010.

Chimenos, J.M., Fernández, A.I., Cervantes, A., Miralles, L., Fernández, M.A., Espiel, F., 2005. Optimizing the APC residue washing process to minimize the release of chloride and heavy metals. Waste Manag. 25 (7), 686–693. https://doi.org/10.1016/j.wasman.2004.12.014.

Costa, G., 2009. Accelerated carbonation of minerals and industrial residues for carbon dioxide storage. PhD thesis. Università Degli Studi Di Roma, Rome.

Crystallography Open Database, 2021. COD: Search. http://www.crystallography.net (accessed 20 January 2021).

Dimech, C., Cheeseman, C., Cook, S., Simon, J., Boccaccini, A., 2008. Production of sintered materials from air pollution control residues from waste incineration. J. Mater. Sci. 43, 4143–4151. https://doi.org/10.1007/s10853-007-2166-9.

Dontriros, S., Likitlersuang, S., Janjaroen, D., 2020. Mechanisms of chloride and sulfate removal from municipal-solid-waste-incineration fly ash (MSWI FA): effect of acid-base solutions. Waste Manag. 101, 44–53. https://doi.org/10.1016/j.wasman.2019.09.033.

Ecke, H., Menad, N., Lagerkvist, A., 2002. Treatment-oriented characterization of dry scrubber residue from municipal solid waste incineration. J. Mater. Cycles Waste Manage. 4, 117–126. https://doi.org/10.1007/s10163-001-0063-x.

Engineering Notes, 2023. Effect of Chloride Attack on Durability of Concrete - Concrete Technology. https://www.engineeringenotes.com/concrete-technology/durability/effect-of-chloride-attack-on-durability-of-concrete-concrete-technology/32209 (accessed 30 August 2023).

European Union, 2003. 2003/33/EC: Council Decision of 19 December 2002 establishing criteria and procedures for the acceptance of waste at landfills pursuant to Article 16 of and Annex II to Directive 1999/31/EC: http://data.europa.eu/eli/dec/2003/33(1)/oj (accessed 12 November 2020).

European Union, 2023. 2000/532/EC: Commission Decision of 3 May 2000 replacing Decision 94/3/EC establishing a list of wastes pursuant to Article 1(a) of Council Directive 75/442/EEC on waste and Council Decision 94/904/EC establishing a list of hazardous waste pursuant to Article 1(4) of Council Directive 91/689/EEC on hazardous waste (notified under document number C(2000) 1147) (Text with EEA relevance) (2000/532/EC)Text with EEA relevance. http://data.europa.eu/eli/dec/2000/532/2023-12-06 (accessed 10 January 2024).

Fan, C., Wang, B., Ai, H., Liu, Z., 2022. A comparative study on characteristics and leaching toxicity of fluidized bed and grate furnace MSWI fly ash. J. Environ. Manage. 305, 1143–1145. https://doi.org/10.1016/j.jenvman.2021.114345.

Fernández Bertos, M., Li, X., Simons, S., Hills, C., Carey, P., 2004a. Investigation of accelerated carbonation for the stabilisation of MSW incinerator ashes and the sequestration of $CO_2$. Green Chem. 6, 428–436. https://doi.org/10.1039/B401872A.

Fernández Bertos, M., Scuzzarella, A., Simons, S., Hills, C., Carey, P., 2004b. Kinetic Study of the Accelerated Carbonation of MSW Incinerator Air Pollution Control Residues. Proc. AIChE Annual Meeting. https://www.academia.edu/64505218.

Geysen, D., Vandecasteele, C., Jaspers, M., Wauters, G., 2004. Comparison of immobilisation of air pollution control residues with cement and with silica. J. Hazard. Mater. 107 (3), 131–143. https://doi.org/10.1016/j.jhazmat.2003.12.001.

Ghouleh, Z., Shao, Y., 2018. Turning municipal solid waste incineration into a cleaner cement production. J. Clean. Prod. 195, 268–279. https://doi.org/10.1016/j.jclepro.2018.05.209.

Grazulis, S., Chateigner, D., Downs, R.T., Yokochi, A.F.T., Quiros, M., Lutterotti, L., Manakova, E., Butkus, J., Moeck, P., Le Bail, A., 2009. Crystallography Open Database - an open collection of crystal structures. J. Appl. Cryst. 42, 726–729. https://doi.org/10.1107/S0021889809016690.

Gunning, P. J., Hills, C. D., Carey, P., 2011. Novel approaches to the valorisation of ashes using aggregation by carbonation. Second International Slag Valorisation Symposium, Leuven. https://www.researchgate.net/publication/228511247.

Han, S., Song, Y., Ju, T., Meng, Y., Meng, F., Song, M., Lin, L., Liu, M., Li, J., Jiang, J., 2022. Recycling municipal solid waste incineration fly ash in super-lightweight aggregates by sintering with clay and using SiC as bloating agent. Chemosphere 307, 135895. https://doi.org/10.1016/j.chemosphere.2022.135895.

He, P.J., Zhang, H., Zhang, C.G., Lee, D.J., 2004. Characteristics of air pollution control residues of MSW incineration plant in Shanghai. J. Hazard. Mater. 116 (3), 229–237. https://doi.org/10.1016/j.jhazmat.2004.09.009.

Heu, R., Shahbazmohamadi, S., Yorston, J., Capeder, P., 2019. Target material selection for sputter coating of SEM samples. Microscopy Today. 27 (4), 32–36. https://doi.org/10.1017/S1551929519000610.

Hjelmar, O., 1996. Disposal strategies for municipal solid waste incineration residues. J. Hazard. Mater. 47 (1–3), 345–368. https://doi.org/10.1016/0304-3894(95)00111-5.

Hu, S.-H., 2005. Stabilization of heavy metals in municipal solid waste incineration ash using mixed ferrous/ferric sulfate solution. J. Hazard. Mater. 123 (1–3), 158–164. https://doi.org/10.1016/j.jhazmat.2005.03.044.

Huang, W.-J., Chu, S.-C., 2003. A study on the cementlike properties of municipal waste incineration ashes. Cem. Concr. Res. 33 (11), 1795–1799. https://doi.org/10.1016/S0008-8846(03)00203-5.

Karlfeldt Fedje, K., Ekberg, C., Skarnemark, G., Steenari, B.M., 2010. Removal of hazardous metals from MSW fly ash—An evaluation of ash leaching methods. J. Hazard. Mater. 173 (1–3), 310–317. https://doi.org/10.1016/j.jhazmat.2009.08.094.

Keppert, M., Siddique, J.A., Pavlík, Z., Herný, R., 2015. Wet-treated MSWI fly ash used as supplementary cementitious material. Adv. Mater. Sci. Eng. 2015, 842807. https://doi.org/10.1155/2015/842807.

Lee, P., Nasserzadeh, V., Swithenbank, J., Laming, J., Goodfellow, J., McLeod, C., Argent, B., Lawrence, D., Garrod, N., 1999. Sintering of the APCr residue from municipal solid waste incinerators. Process Saf. Environ. Prot. 77 (4), 212–218. https://doi.org/10.1205/095758299530099.

Li, J.-s., Xue, Q., Fang, L., Poon, C., 2017. Characteristics and metal leachability of incinerated sewage sludge ash and air pollution control residues from Hong Kong evaluated by different methods. Waste Manag. 64, 161–170. https://doi.org/10.1016/j.wasman.2017.03.033.

Li, M., Xiang, J., Hu, S., Sun, L.S., Su, S., Li, P.S., Sun, X.X., 2004. Characterization of solid residues from municipal solid waste incinerator. Fuel 83 (10), 1397–1405. https://doi.org/10.1016/j.fuel.2004.01.005.

Newbury, D.E., Ritchie, N.W., 2013. Is scanning electron microscopy/energy dispersive X-ray spectrometry (SEM/EDS) quantitative? Scanning 35 (3), 141–168. https://doi.org/10.1002/sca.21041.

Nikravan, M., Ramezanianpour, A.A., Maknoon, R., 2020. Study on physiochemical properties and leaching behavior of residual ash fractions from a municipal solid waste incinerator (MSWI) plant. J. Environ. Manage. 260, 110042. https://doi.org/10.1016/j.jenvman.2019.110042.

Oxford Instruments NanoAnalysis, 2022. AZtecLive. https://nano.oxinst.com/products/azteclive.

Quina, M.J., Santos, R.C., Bordado, J.C., Quinta-Ferreira, R.M., 2008. Characterization of air pollution control residues produced in a municipal solid waste incinerator in Portugal. J. Hazard. Mater. 152 (2), 853–869. https://doi.org/10.1016/j.jhazmat.2007.07.055.

Quina, M.J., Bordado, J.C., Quinta-Ferreira, R.M., 2009. The influence of pH on the leaching behaviour of inorganic components from municipal solid waste APC residues. Waste Manag. 29, 2483–2493. https://doi.org/10.1016/j.wasman.2009.05.012.

Ranjbar, N., Kuenzel, C., 2017. Cenospheres: a review. Fuel 207, 1–12. https://doi.org/10.1016/j.fuel.2017.06.059.

Rigaku Corporation, 2021. Rigaku PDXL (Version 2.3). https://rigaku-pdxl.software.informer.com/2.3/.

Roberts, L.J., Mason, P.E., Jones, J.M., Gale, W.F., Williams, A., Hunt, A., Ashman, J., 2019. The impact of aluminosilicate-based additives upon the sintering and melting behaviour of biomass ash. Biomass Bioenergy 127, 105284. https://doi.org/10.1016/j.biombioe.2019.105284.

Robinson, H., Knox, K., Formby, R., Bone, B., 2004. Testing of residues from incineration of municipal solid waste, Science Report P1-494/SR2. Environment Agency, Bristol. https://www.gov.uk/government/publications/testing-of-residues-from-incineration-of-municipal-solid-waste.

Sabbas, T., Polettini, A., Pomi, R., Astrup, T., Hjelmar, O., Mostbauer, P., Cappai, G., Magel, G., Salhofer, S., Speiser, C., Heuss-Assbichler, S., Klein, R., Lechner, P., 2003. Management of municipal solid waste incineration residues. Waste Manag. 23 (1), 61–88. https://doi.org/10.1016/S0956-053X(02)00161-7.

Sawell, S.E., Chandler, A.J., Eighmy, T.T., Hartlén, J., Hjelmar, O., Kosson, D., Van Der Sloot, H., Vehlow, J., 1995. An international perspective on the characterisation and management of residues from MSW incinerators. Biomass Bioenergy 9 (1–5), 377–386. https://www.sciencedirect.com/science/article/pii/0961953495001050?via%3Dihub.

Singh, G., Kumari, B., Kitri, G.S., Kumar, N., Mallick, S., 2018. Fluoride distribution and contamination in the water, soil and plants continuum and its remedial technologies, an Indian perspective - a review. Environ. Pollut. 239, 95–108. https://doi.org/10.1016/j.envpol.2018.04.002.

Song, G.-J., Kim, K.-H., Yong-Chil, S., Sam-Cwan, K., 2004. Characteristics of ashes from different locations at the MSW incinerator equipped with various air pollution control devices. Waste Manag. 24 (1), 99–106. https://doi.org/10.1016/S0956-053X(03)00073-4.

Statista, 2025. Number of waste to energy plants in the United Kingdom from 2010 to 2022. https://www.statista.com/statistics/1619424/waste-to-energy-plants-in-the-united-kingdom/ (accessed 8 December 2025).

Sun, J., Fernández Bertos, M., Simons, S.J., 2008. Kinetic study of accelerated carbonation of municipal solid waste incinerator air pollution control residues for sequestration of flue gas $CO_2$. Energy Environ. Sci. 1 (13), 370–377. https://doi.org/10.1039/B804165M.

Tolvik Consulting Ltd., 2016. UK Energy from Waste Statistics - 2015. Tolvik Consulting Ltd., Dursley. https://www.tolvik.com/published-reports/view/uk-energy-from-waste-statistics-2015/.

Tolvik Consulting Ltd., 2017. UK Energy from Waste Statistics - 2016. Tolvik Consulting Ltd., Dursley. https://www.tolvik.com/published-reports/view/uk-energy-from-waste-statistics-2016/.

Tolvik Consulting Ltd., 2021. UK Energy from Waste Statistics - 2020. Tolvik Consulting Ltd., Dursley. https://www.tolvik.com/published-reports/view/uk-energy-from-waste-statistics-2020/.

Tolvik Consulting Ltd., 2024. UK Energy from Waste Statistics - 2023. Tolvik Consulting Ltd., Somerset. https://www.tolvik.com/published-reports/view/uk-energy-from-waste-statistics-2023/.

Wiles, C.C., 1996. Municipal solid waste combustion ash: State-of-the-knowledge. J. Hazard. Mater. 47, 325–344. https://doi.org/10.1016/0304-3894(95)00120-4.

Xia, P., 2021. Stories: Environmental Impacts of Chloride Contamination. https://storymaps.arcgis.com/stories/f998c640cc7d4fc9bca0d0aba8adffeb (accessed 21 August 2023).

Yang, Z., Tian, S., Ji, R., Liu, L., Wang, X., Zhan, Z., 2017. Effect of water-washing on the co-removal of chlorine and heavy metals in air pollution control residue from MSW incineration. Waste Manag. 68, 221–231. https://doi.org/10.1016/j.wasman.2017.06.039.

Zhao, Y., Zhang, J.Y., Gao, Q., Guo, X., Zheng, C.G., 2006. Chemical composition and evolution mechanism of ferrospheres in fly ash from coal combustion. Proc. CSEE 26, 82–86. https://www.researchgate.net/publication/289435356.